

# Cations Affect the Rate of Gating Charge Recovery in Wild-type and W434F *Shaker* Channels through a Variety of Mechanisms

ZOLTAN VARGA,<sup>1,3</sup> MARTIN D. RAYNER,<sup>1,2</sup> and JOHN G. STARKUS<sup>1</sup>

<sup>1</sup>Békésy Laboratory of Neurobiology, Pacific Biomedical Research Center, and <sup>2</sup>School of Medicine, University of Hawaii, Honolulu, HI 96822

<sup>3</sup>Department of Biophysics and Cell Biology, Medical and Health Science Center, University of Debrecen, 4012 Debrecen, Hungary

**ABSTRACT** In this study we examine the effects of ionic conditions on the gating charge movement in the fast inactivation-removed wild-type *Shaker* channel and its W434F mutant. Our results show that various ionic conditions influence the rate at which gating charge returns during repolarization following a depolarizing pulse. These effects are realized through different mechanisms, which include the regulation of channel closing by occupying the cavity, the modulation of transitions into inactivated states, and effects on transitions between closed states via a direct interaction with the channel's gating charges. In generating these effects the cations act from the different binding sites within the pore. Ionic conditions, in which conducting wild-type channels close at different rates, do not significantly affect the rate of charge recovery upon repolarization. In these conditions, channel closing is fast enough not to be rate-limiting in the charge recovery process. In the permanently P-inactivated mutant channel, however, channel closing becomes the rate-limiting step, presumably due to weakened ion-ion interactions inside the pore and a slower intrinsic rate of gate closure. Thus, variations in closing rate induced by different ions are reflected as variations in the rate of charge recovery. In 115 mM internal Tris<sup>+</sup> and external K<sup>+</sup>, Cs<sup>+</sup>, or Rb<sup>+</sup>, low inward permeation of these ions can be observed through the mutant channel. In these instances, channel closing becomes slower than in Tris<sup>+</sup><sub>o</sub>/Tris<sup>+</sup><sub>i</sub> solutions showing resemblance to the wild-type channel, where higher inward ionic fluxes also retard channel closing. Our data indicate that cations regulate the transition into the inactivated states from the external lock-in site and possibly the deep site. The direct action of barium on charge movement is probably exerted from the deep site, but this effect is not very significant for monovalent cations.

**KEY WORDS:** potassium channels • gating current • barium • P-inactivation • C-inactivation

## INTRODUCTION

Potassium channels are highly selective for K<sup>+</sup>, but can pass other ions like Rb<sup>+</sup> and Cs<sup>+</sup> or even Na<sup>+</sup> in the absence of these other ions (Korn and Ikeda, 1995; Starkus et al., 1997). The ionic species and concentrations on the two sides of the membrane have long been known to affect channel gating. These include effects on slow inactivation (Hoshi et al., 1991; Lopez-Barneo et al., 1993; Baukrowitz and Yellen, 1995, 1996; Levy and Deutsch, 1996; Starkus et al., 1997), on deactivation (Swenson and Armstrong, 1981; Matteson and Swenson, 1986; Demo and Yellen, 1992), and on the recovery rates of gating charge (Chen et al., 1997; Wang et al., 1999). A foot-in-the-door type mechanism was suggested to explain the effect of cations on both deac-

tivation and slow inactivation, according to which neither of these processes could proceed while a permeating ion was occupying a binding site in the pore (Demo and Yellen, 1992; Baukrowitz and Yellen, 1995, 1996; Kiss and Korn, 1998; Melishchuk and Armstrong, 2001). The site responsible for regulating the rate of slow inactivation is likely to be different from the one controlling the rate of deactivation.

In Kv1.5 channels, the permeating ions K<sup>+</sup> and Cs<sup>+</sup> were found to accelerate the return of gating charge when compared with conditions where no permeant ions were present (Chen et al., 1997). The results of Wang et al. (1999) showed substantial differences in the rate of charge return (OFF gating current decay) in various ionic conditions in the nonconducting mutant W472F of the Kv1.5 channel (equivalent of *Shaker* W434F). Intracellular cations were significantly more effective at regulating the rate of gating charge return than extracellular cations. This series of studies suggests a possible allosteric modulation of K<sup>+</sup> channel deactivation by permeant ions, but favors the hypothesis that accelerated slow inactivation in the absence of permeant ions is the major cause of the slowing of gating charge return.

External Ba<sup>2+</sup> was also shown to accelerate OFF gat-

Address correspondence to John G. Starkus, Bekesy Lab of Neurobiology, University of Hawaii, 1993 East-West Rd., Honolulu, HI 96822. Fax: (808) 956-6984; E-mail: john@pbrc.hawaii.edu

Portions of this work were previously published in abstract form (Varga, Z., M.D. Rayner, and J.G. Starkus. 2001. *Biophys. J.* 80(1):217a (Abstr.); Starkus, J.G., Z. Varga, and M.D. Rayner. 2001. *Biophys. J.* 80(1):218a (Abstr.)).

ing currents in wild-type and W434F mutant *Shaker* channels (Hurst et al., 1997). The interpretation of the results was that bound  $\text{Ba}^{2+}$  increases the backward and/or decreases the forward rates of transitions between two closed states late in the activation pathway, thereby destabilizing the open state of the channel.

In this study we attempt to shed light on the mechanism by which these ionic conditions influence the return of gating charge. In our model we build on the generally accepted view that the channel contains three, four, or possibly even more binding sites for the  $\text{K}^+$  ion within the pore (Stampe and Begenisich, 1996; Doyle et al., 1998; Harris et al., 1998; Jiang and MacKinnon, 2000; Thompson and Begenisich, 2001). There are three putative binding sites within the short stretch of the selectivity filter. The one at the innermost end of the filter is called the “deep” or “high affinity” site, which is believed to be highly selective for  $\text{K}^+$ . It was also shown by X-ray crystallography to be the binding site for  $\text{Ba}^{2+}$  (Jiang and MacKinnon, 2000). The site just external to it was named “enhancement” site by Neyton and Miller (1988a,b). This site was also found to be highly selective for  $\text{K}^+$ , but it was shown to have a very low affinity for  $\text{K}^+$  in the range of hundreds of millimoles. Two other sites on either end of the selectivity filter were termed “external and internal lock-in” sites according to which side of the high affinity site they are located on. The external lock-in site shows high affinity and selectivity, whereas the internal lock-in site has lower affinity and displays little selectivity. The internal lock-in site is assumed to be in the wider cavity internal to the selectivity filter (Jiang and MacKinnon, 2000). Here the ions are hydrated and are not in close contact with the channel protein.

Recently, Melishchuk and Armstrong (2001) have found that the size of the internal cavity in the *Shaker* channel pore, which was changed by mutations at position 470, determined what ions could be trapped inside the cavity by the closing gate. Studying the OFF gating current kinetics using different cavity sizes and ions, they came to the conclusion that the gate in the wild-type channel cannot close, even if small permeating ions occupy the cavity. They suggest that the slow kinetics of the OFF gating current are due to the slow rate of ions leaving the cavity. This model serves as a starting point in our investigation.

Our study aims at clarifying how various cations affect gating charge return. Is it an indirect effect via the modulation of channel closing rate, is it a direct coupling between the ions in the pore and the gating charges of the protein, are inactivated states involved, or is it the combination of all these effects? How are these phenomena different in the nonconducting W434F mutant from the wild-type channel, and what causes these differences? The ion at which binding site

has the greatest influence on channel closing and charge recovery? These are questions we seek to answer in this paper. The model proposed by Melishchuk and Armstrong (2001) combined with models on the effect of inactivated states on charge recovery from Wang et al. (1999, 2000) and Wang and Fedida (2001) and models of electrostatic interactions of ions inside the pore can account for most of the described effects of ions on gating charge return.

## MATERIALS AND METHODS

### Oocyte Preparation, Injection, and Incubation

Oocytes were obtained from female *Xenopus laevis* using standard techniques which have been described previously in detail (Iversen and Rudy, 1990; Stuhmer, 1992). Briefly, oocytes were removed from the frog and then collagenased in  $\text{Ca}^{2+}$ -free medium to separate the eggs and remove the follicular layer. Healthy, stage V, eggs were selected and subsequently injected 6–18 h after collagenasing using a Drummond nanoinjector (Drummond Scientific Co.), with ~50 nl of RNA diluted to different concentrations depending on the desired level of expression. For high levels of expression necessary for gating measurements, we normally used a 1:1 dilution of RNA. After injection, oocytes are incubated and agitated at 18°C in ND-96 plus 0.2% gentamicin, 2.5% sodium pyruvate, and 1% horse serum (Quick and Lester, 1994). Oocytes were incubated 1–2 d before electrophysiological recordings.

### Channel Expression

In this study two types of *Shaker* potassium channel were used, namely, the wild-type (WT)\* and the “nonconducting” mutant, W434F. The WT channel is the *Shaker* D 29-4 construct (Iversen and Rudy, 1990). Within this construct the fast, N-type inactivation has been removed by deletion of the residues 2–29 (McCormack et al., 1994). This inactivation-removed construct has been referred to previously as Sh  $\Delta$  or Sh IR. In this study, we refer to this construct as the WT channel. In the same WT background, a single point mutation of a tryptophan to a phenylalanine at position 434, W434F, was also used here (Perozo et al., 1993).

### Recording and Simulation of Ionic and Gating Currents

Prior to recording from macropatches, the vitelline membrane was removed manually with blunt Dumont forceps after treating the oocyte for a few minutes in a hyperosmolar medium (Methfessel et al., 1986). Patch pipettes were made from aluminosilicate glass (Hilgenberg) pulled to a tip diameter of 3–4  $\mu\text{m}$ . To reduce noise and increase clamp speed, the glass capacitance was reduced by coating the glass with dental wax and raising the patch pipette as close as possible to the bath surface. Prior to patching, the glass tip was fire-polished on a Narashige microforge (Narashige). Recordings were obtained using an EPC-9 amplifier (HEKA Elektronik) driven by the Pulse program (HEKA Elektronik). Linear and capacitive currents were subtracted from the data online by using a variable P/n procedure (Heinemann et al., 1992). The filter frequency during data acquisition was set to 1/5 of the sampling frequency. Traces were further filtered during analysis. Data averaging and analysis were performed using Pulse-

\*Abbreviations used in this paper: NFR, normal frog ringer;  $\text{NMG}^+$ , N-methyl-D-glucamine; Q-V, charge-voltage; WT, wild-type.

Tools, PulseFit (HEKA Elektronik), and Igor (Wavemetrics) software.

### Solutions

In addition to monovalent chloride salt, external ("Ringer") solutions always contained 1.8 mM  $\text{CaCl}_2$  and 10 mM HEPES (pH 7.2). Internal ("EGTA") solutions contained 1.8 mM EGTA and 10 mM HEPES (pH 7.2). The solutions were named according to their monovalent cation content. External solutions contained (in mM): normal frog ringer (NFR), 115 NaCl, 2.5 KCl; K-Ringer, 115 KCl; Na-Ringer, 115 NaCl; Tris-Ringer, 115 TrisCl; Rb-Ringer, 115 RbCl; Cs-Ringer, 115 CsCl. Internal solutions contained (in mM): K-Egta, 115 KCl; Na-Egta, 115 NaCl; Tris-Egta, 115 TrisCl; Rb-Egta, 115 RbCl; Cs-Egta, 115 CsCl. Internal and external solutions containing 1 mM of  $\text{K}^+$ ,  $\text{Cs}^+$ ,  $\text{Rb}^+$ , or  $\text{Na}^+$  contained 115 mM  $\text{Tris}^+$  as the substitute ion. In the text and figures, the solutions are only specified by the concentrations of the monovalent cations: external//internal solutions. No  $\text{CaCl}_2$  was added to external solutions containing  $\text{Ba}^{2+}$  to avoid unnecessary increases in the ionic strength of the solution. All experiments were performed at room temperature of 22–24°C. Solution exchanges were achieved by a gravity-driven perfusion system. Excised inside-out or outside-out macropatches were positioned in front of the outlet of the perfusion head.

### RESULTS

#### Rates of Charge Recovery Differ in Wild-type and W434F Channels

Fig. 1 presents typical data recordings obtained in this study and the voltage protocol used to elicit these current traces. To measure gating currents in the highly conducting wild-type channel, the concentration of permeating ions ( $\text{K}^+$ ,  $\text{Rb}^+$ ) was lowered to 1 mM to reduce conductance. Second, we used symmetrical solutions ( $E_{\text{rev}} = 0$  mV) and applied a double pulse protocol. A pair of pulses to the reversal potential generates an ON gating current at 0 mV and the gating current in the second pulse recovers as the duration of the interval of the repolarizing pulse to  $-100$  mV separating the depolarizing pulse increases. Using symmetrical ionic conditions allowed us to simultaneously measure gating currents at 0 mV without a net flow of ionic current (reversal potential) and a tail ionic current at  $-100$  mV. Therefore, within each dataset we could compare the

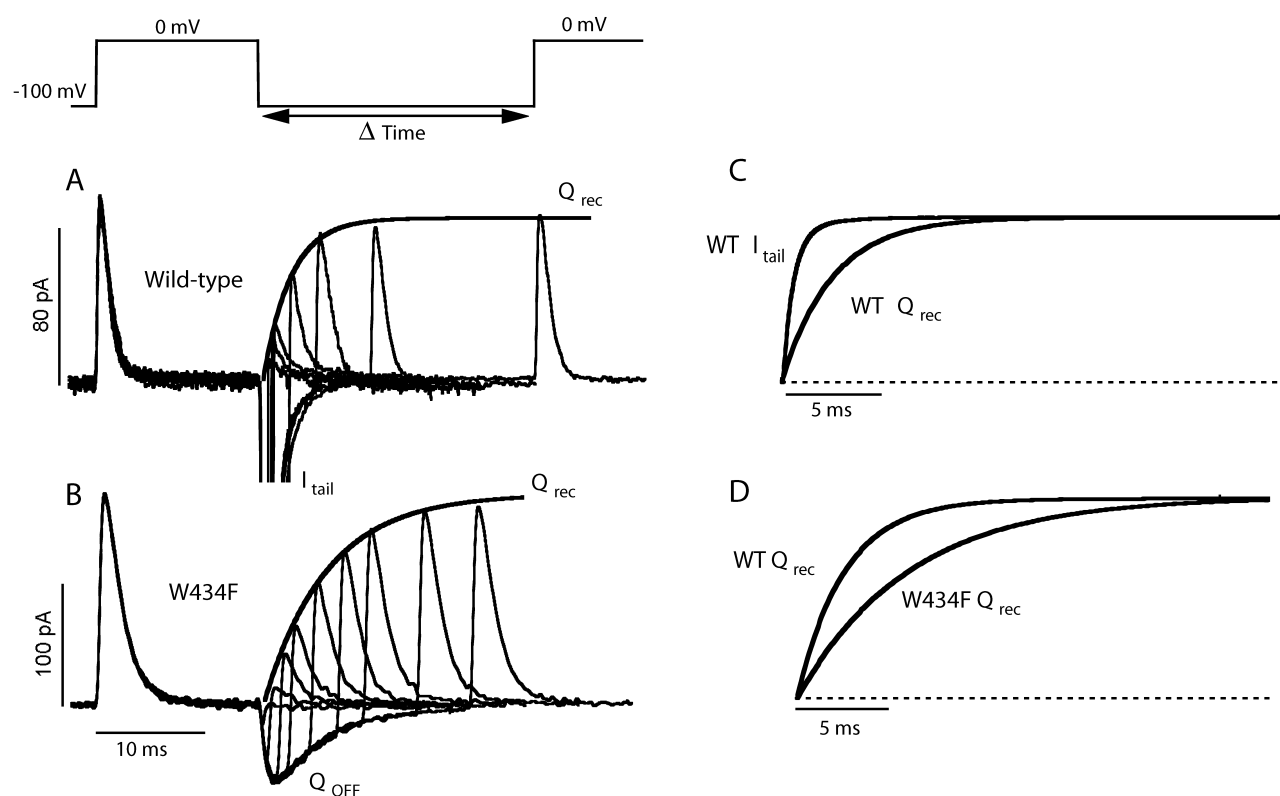
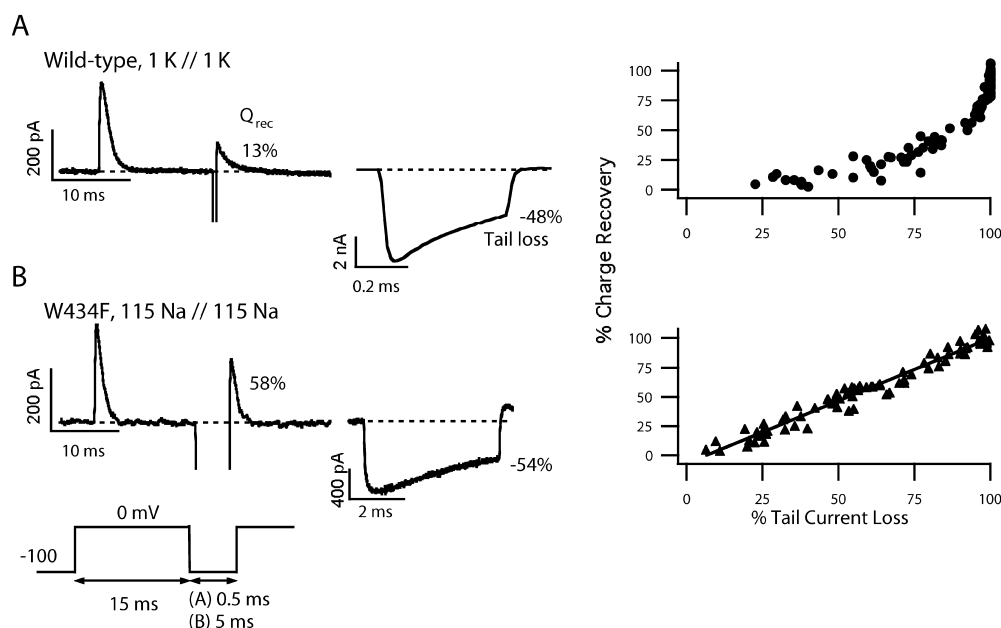


FIGURE 1. Rate of gating charge recovery in wild-type and W434F mutant channels. The rate of charge recovery was assessed by using a double pulse protocol. A pair of pulses to 0 mV was applied to inside-out patches separated by varying durations at  $-100$  mV. Both the external and internal solutions contained 1 mM  $\text{K}^+$  + 115 mM  $\text{Tris}^+$  to achieve a reversal potential of 0 mV. (A) The depolarizing pulse to 0 mV evokes an ON gating current, then large inward tail currents are seen through the wild-type channels during the repolarizing pulse, and the ON gating current in the second pulse recovers with increasing interpulse durations. (B) Only the OFF gating current is present in the nonconducting mutant during repolarization. (C) Direct comparison of the rate of tail current decay and that of charge recovery in the wild-type channel indicates that channel closing is fast compared with charge return. The actual normalized tail current trace and the fit to the recovering second ON gating currents from A are shown. (D) Charge recovery is significantly faster in the wild-type channels ( $\tau = 2.5$  ms for this patch) than in the W434F mutant ( $\tau = 5.9$  ms for this patch). The fits were taken from A and B and are shown normalized for direct comparison.



Na<sup>+</sup> solutions. In the wild-type, 13% of the charge recovered (A, left) while the tail current dropped 48% compared with its peak value (A, middle) in this patch; however, (B) in W434F a tail current loss of 54% was accompanied by 58% charge recovery. These results from many patches (WT:  $n = 29$ ; W434F:  $n = 18$ ) and various interpulse durations are summarized in the point plots (right).

rate of channel closure (from the tail currents) with the rate of charge recovery (from gating currents in the second pulse).

In Fig. 1, the rates of charge recovery are compared for the conducting wild-type (Fig. 1 A) and the “non-conducting” mutant W434F channel (Fig. 1 B) in symmetrical 1 mM K<sup>+</sup> conditions using the impermeant Tris<sup>+</sup> as a substitute cation. Fig. 1 C clearly illustrates that the rate of tail current decay is considerably faster than the rate of charge recovery in the wild-type channel. Direct comparison of the two channel types in Fig. 1 D reveals that gating charge recovers significantly more quickly in the wild-type channel than in the mutant (single exponential charge recovery time constants:  $2.80 \pm 0.23$  ms for wild-type,  $n = 29$ , and  $7.99 \pm 0.52$  ms for W434F,  $n = 15$ ,  $P < 2 \times 10^{-9}$ ). This difference in charge recovery rates can originate from the first transition between the open state and closed state during deactivation or from transitions between closed states later in the deactivation pathway associated with most of the charge movement. The involvement of inactivated states beyond the open state from which recovery is slow may also be possible. Our experiments address this question as well as how different cation species affect charge recovery rates and how these effects are different in the two channel types.

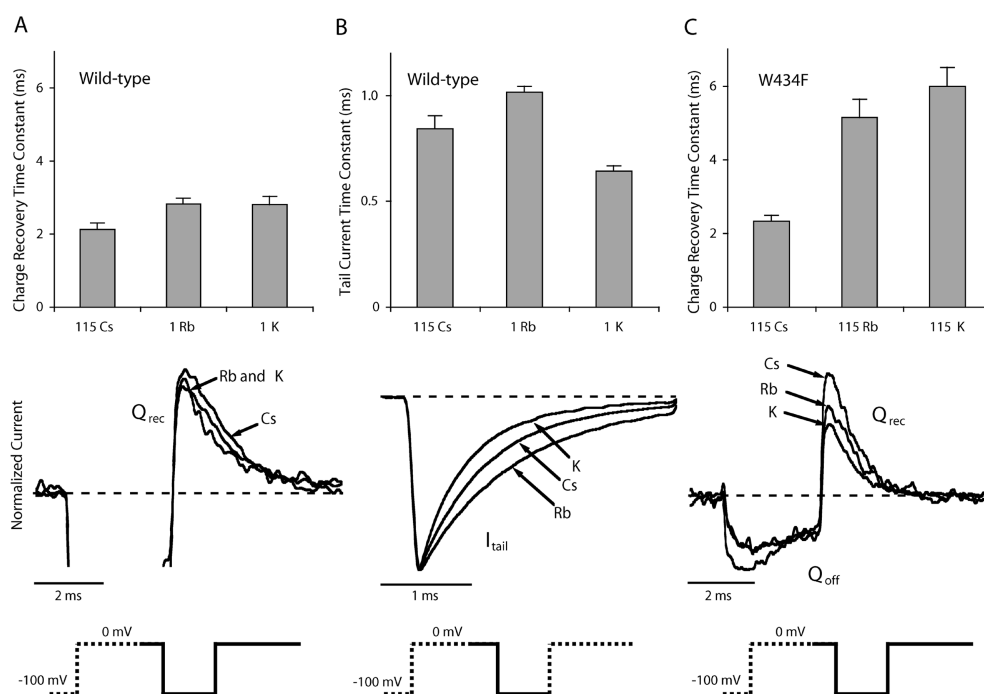
#### Relationship between Channel Closing and Charge Recovery

To investigate these questions we first compared the fraction of channels closed (percentage tail current

loss) with the fraction of total charge recovered during a repolarizing pulse and found that this relationship appears to be different in the two channel types (Fig. 2, A and B). The percentage of the channels that closed during the repolarizing pulse was determined from the decay of the ionic current. The ratio of integrated gating charge in the second pulse to that in the first pulse yielded the fraction of total gating charge that returned during the repolarizing pulse. For wild-type channels, Fig. 2 A shows that a significant fraction of channels closes before any significant fraction of gating charge recovers in symmetrical 1 K<sup>+</sup> solutions. A plot of the percentage of recovered gating charge against the percentage of channels that closed during the repolarizing step reveals a clearly nonlinear relationship. This finding is consistent with the behavior of linear models of deactivation, in which the first channel-closing step carries little charge and is considerably faster than the subsequent charge carrying steps between closed states (Bezanilla et al., 1994). This relationship in the wild-type channel would predict that certain experimental conditions, which influence channel closure, may not necessarily affect the rates of charge recovery.

To be able to measure the rate of tail current decay in the mutant channel the use of Na<sup>+</sup> solutions was necessary, since the other ions used in this study do not significantly permeate through W434F. Moreover, for Na<sup>+</sup> conduction to occur, ions that normally permeate through the wild-type channel (e.g., K<sup>+</sup> ions) have to be removed so that they do not block the Na<sup>+</sup> current.

FIGURE 2. Relationship between gating charge recovery and channel closure in the wild-type and the W434F channel. The percentage of gating charge recovery was determined using the double pulse protocol by calculating the ratio of the ON gating charge in the second pulse to that in the first pulse (left). Tail currents from the left panels are shown on the middle panels on a different time scale. Solutions used in the experiments were (A) symmetrical 1 K<sup>+</sup> + 115 Tris<sup>+</sup> for wild-type and (B) symmetrical 115 Na<sup>+</sup> for W434F channels. (A) In the wild-type channel the relationship between charge recovery and channel closing is nonlinear in 1 K<sup>+</sup> solutions, (B) but it is linear in the W434F mutant in 115



time constants show a strong dependence on the ionic species in the W434F mutant. (C, middle) Recovery of gating currents in the indicated solutions from different patches is sensitive to ion species. Symmetrical solutions were used, and labels indicate the main cation and its concentration in mM. In 1 mM  $K^+$  and 1 mM  $Rb^+$  solutions, the substitute ion was 115 mM  $Tris^+$ . Bars indicate the mean  $\pm$  SEM of single exponential time constants determined for individual patches. The number of patches was as follows, wild-type: 115  $Cs^+$ ,  $n = 16$ ; 1  $Rb^+$ ,  $n = 22$ ; 1  $K^+$ ,  $n = 29$ . W434F: 115  $Cs^+$ ,  $n = 8$ ; 115  $Rb^+$ ,  $n = 10$ ; 115  $K^+$ ,  $n = 15$ .

In contrast to the wild-type, the plot for the W434F mutant channel in symmetrical 115  $Na^+$  solutions indicates a linear relationship between the rates of channel closing and gating charge recovery (Fig. 2 B). Such a strict relationship can be explained if channel closing becomes so slow that it becomes the rate-limiting step in the charge recovery process. Alternatively, the slow recovery from an inactivated state beyond the open state could also be responsible for the direct link between the two quantities. This direct link predicts that conditions which affect channel closure (or the recovery from the inactivated state) will necessarily affect the rate of charge movement.

The results shown in Fig. 3 confirm these predictions. We measured the rates of gating charge recovery and tail current decay in symmetrical solutions containing  $K^+$ ,  $Rb^+$ , or  $Cs^+$  using the double pulse protocol described for Fig. 1. The concentration of the cations used in these experiments (1 or 115 mM) was chosen such that we would be able to measure tail current kinetics in the wild-type channel without ionic current contamination in the gating current, and such that we would obtain meaningful charge recovery time constants in the mutant channel (for further explanation see DISCUSSION). For easy comparison, we characterized these quantities by single exponential time constants, even though the presence of a small slow com-

ponent was evident in most conditions (see below). In the wild-type channel, various ionic conditions showing very similar charge recovery rates (Fig. 3 A,  $P = 0.07$ , ANOVA) produced significantly different tail current kinetics (Fig. 3 B,  $P < 2.2 \times 10^{-9}$ , ANOVA). For example, tail current decay was much slower in 1  $Rb^+$  solutions than in 1  $K^+$  solutions (time constants:  $Rb^+$ ,  $1017 \pm 28 \mu s$ ,  $n = 22$ ;  $K^+$ ,  $643 \pm 26 \mu s$ ,  $n = 29$ ;  $P < 2.4 \times 10^{-12}$ ), whereas gating charge returned at the same rate (time constants:  $Rb^+$ ,  $2.82 \pm 0.16$  ms;  $K^+$ ,  $2.80 \pm 0.23$  ms;  $P = 0.94$ ). Fig. 3 A, middle, illustrates the similar amounts of ON gating charge in the second pulse of the double pulse protocol in the presence of these ions. The traces were normalized by the peak of the ON gating current in the first pulse. The varying tail current decay rates are shown in Fig. 3 B, middle. Tail currents were normalized by their peaks and are part of the same traces that are shown in Fig. 3 A. The charge recovery rate in symmetrical 115  $Cs^+$  solutions was slightly, but noticeably, faster than in the other two conditions (time constant:  $2.13 \pm 0.19$  ms,  $n = 16$ ).

The W434F mutation renders the channel "nonconducting," so no ionic tail currents are observable in symmetrical solutions containing 115 mM  $K^+$ ,  $Cs^+$ , or  $Rb^+$ , but the rate of gating charge recovery can be easily measured. We found that in contrast to the wild-type channel, the charge recovery rate in W434F is strongly depen-

dent on the cation composition of the solutions used (Fig. 3 C,  $P < 6.0 \times 10^{-5}$ , ANOVA). The different amounts of charge in the second ON gating current illustrate this well (Fig. 3 C, middle). These results are consistent with the findings of Wang et al. (1999) on W472F mutant hKv1.5 channels (the analogue of *Shaker* W434F).

These observations imply that ionic effects on the rate of gating charge return are mostly indirect via the modulation of the channel closing rate. It has been shown that differences in the rate of gating charge return between various ionic conditions in the mutant channel only become apparent following depolarizing pulses large enough to open the channels (Wang et al., 1999). Similarly, Perozo et al. (1993) showed slowed OFF gating currents in the presence of internal TEA only after the channels were opened. These results support the idea that the rate-limiting transition that is affected by cations during deactivation is the closing of the internal gate. Thus, cations apparently affect the closing of the gate, and charge recovery is only affected if gate closure is slow enough compared with the subsequent charge carrying steps to become rate-limiting. Of course, any slow backward transition beyond the open state modulated by cations could also be responsible for the observed effects.

Although the above reasoning suggests that channel closing during a repolarizing pulse is slow in W434F, the only direct evidence supporting it came from the symmetrical  $\text{Na}^+$  condition, which is known to be associated with altered channel function and the involvement of inactivated states (Starkus et al., 1997, 1998; Wang et al., 2000; Loboda et al., 2001; Wang and Fedida, 2001). We therefore looked for a more direct way to observe this phenomenon in the presence of  $\text{K}^+$ .

#### *Ion Permeation through W434F Makes Channel Closing Slow*

Even though W434F is labeled “nonconducting,” we discovered small  $\text{K}^+$ ,  $\text{Rb}^+$ , and  $\text{Cs}^+$  currents when large concentration gradients were created. When the external side of outside-out patches was exposed to solutions containing 115 mM of these ions, and the pipette (internal) solution contained 115  $\text{Tris}^+$ , a step to 0 mV elicited outward gating currents followed by small inward ionic currents (Fig. 4 A). The inward ionic currents became more evident during the step back to  $-100$  mV, when the mixture of the OFF gating currents and inward ionic currents resulted in  $Q_{\text{OFF}}/Q_{\text{ON}}$  ratios significantly exceeding one.

Judged by the  $Q_{\text{OFF}}/Q_{\text{ON}}$  ratios,  $\text{Cs}^+$  and  $\text{Rb}^+$  permeation was very low ( $1.15 \pm 0.02$ ,  $n = 5$  and  $1.15 \pm 0.03$ ,  $n = 3$ , respectively), but  $\text{K}^+$  permeation was considerable ( $2.82 \pm 0.27$ ,  $n = 8$ ; Fig. 4 B). Under these conditions, the decay of the tail current was much slower than that seen in the wild-type channel in symmetrical 1  $\text{K}^+$  solutions (W434F:  $13.92 \pm 2.13$  ms,  $n = 8$  and WT:

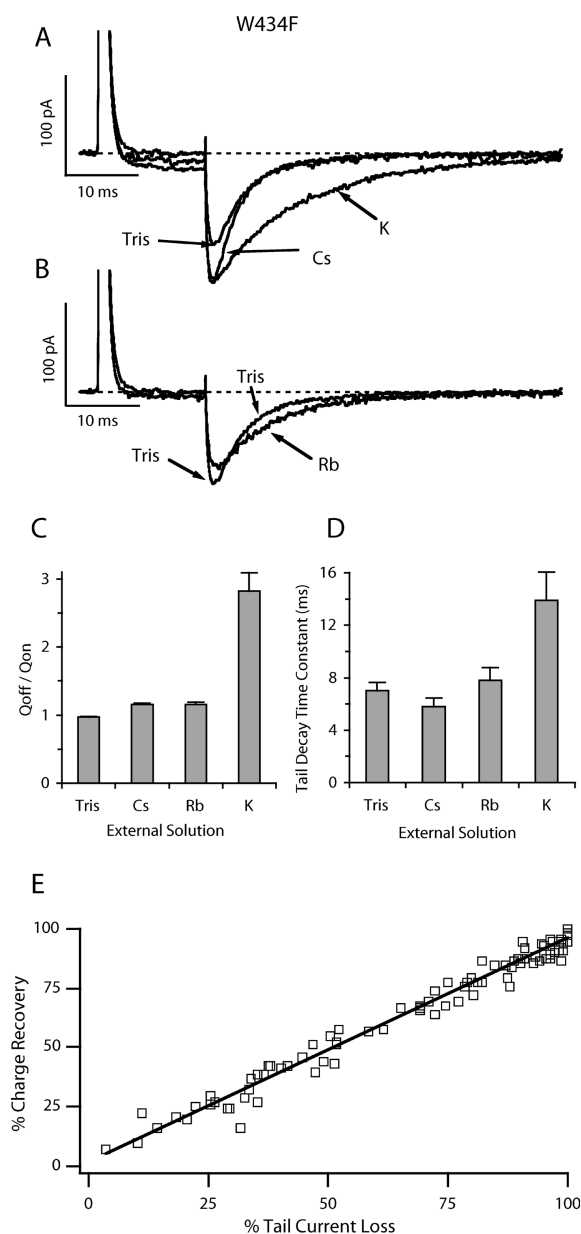


FIGURE 4. Low permeation and slow channel closing in W434F. (A and B) The external side of an outside-out patch was exposed to solutions containing 115 mM  $\text{K}^+$ ,  $\text{Cs}^+$ ,  $\text{Rb}^+$ , or  $\text{Tris}^+$ , whereas the pipette solution (internal solution) contained 115 mM  $\text{Tris}^+$ . Traces on A and B are from the same patch and are only separated for clarity. Currents were elicited by a 15-ms step to 0 mV from a holding potential of  $-100$  mV, followed by a step back to  $-100$  mV. For external  $\text{Tris}^+$ , only the ON and OFF gating currents are seen during depolarizing and repolarizing steps, respectively. By contrast, small inward currents are also seen during the depolarizing step in the other external solutions, which increase to noticeable tail currents during the repolarizing step. (C) The ratio of the integrated charge in the OFF gating + tail current to that in the ON gating current indicates significant permeation only with 115  $\text{K}^+$  in the external solution ( $Q_{\text{OFF}}/Q_{\text{ON}} = 2.82 \pm 0.27$ ,  $n = 8$ ). (D) The decay of the tail current was significantly slower in  $\text{K}^+$  than in other conditions. In other external ions, tail decay rate consistently showed the following sequence:  $\text{Cs}^+ > \text{Tris}^+ > \text{Rb}^+$ , but these differences were not statistically significant. (E) The relationship between gating charge recovery and channel closure in the mutant channel is linear in 115  $\text{K}^+$  or 115  $\text{Tris}^+$  solutions. The figure was prepared as described in the legend to Fig. 2.

$643 \pm 26 \mu\text{s}$ ,  $n = 29$ , respectively; Fig. 4 C). The decay of the current was also consistently slower in external  $\text{Rb}^+$  than in  $\text{Tris}^+$ , which showed no signs of permeation ( $\text{Tris}^+$ :  $Q_{\text{OFF}}/Q_{\text{ON}} = 0.97 \pm 0.01$ ), although this difference was not statistically significant (decay time constants:  $\text{Rb}^+$ :  $7.82 \pm 0.97$ ,  $n = 3$  and  $\text{Tris}^+$ :  $7.00 \pm 0.63$  ms,  $n = 3$ , respectively). This is in contrast with the results of Wang et al. (1999), who found that external  $\text{Rb}^+$  accelerated the OFF gating current compared with  $\text{NMG}^+$ . However, they observed no inward  $\text{Rb}^+$  currents, which may explain the conflicting results. In spite of some  $\text{Cs}^+$  permeation, current decay was slightly faster in external  $\text{Cs}^+$  ( $5.77 \pm 0.67$  ms,  $n = 5$ ) than in external  $\text{Tris}^+$ , but the difference was not significant in this case either ( $P = 0.27$ ). This suggests that permeation alone cannot account for the slow closing of the channel, other ionic effects must also play a role.

The presence of the  $\text{K}^+$  tail current allowed us to directly compare the rates of channel closing and charge return in the W434F mutant without the need to use  $\text{Na}^+$ . The relationship between the two quantities was linear (Fig. 4 E), as in symmetrical  $\text{Na}^+$  solutions (Fig. 2 B). This is in contrast with the nonlinear relationship seen in the wild-type channel during  $\text{K}^+$  conduction (Fig. 2 A).

#### Inactivation Makes the Closing of Wild-type Channels Slow in $\text{Na}^+$ Solutions

As mentioned above, the linear relationship in W434F between channel closing and charge recovery in  $\text{Na}^+$  does not necessarily indicate a rate-limiting channel-closing step, it may be the result of the involvement of

inactivated states. In fact, our earlier observations showed that deactivation kinetics also become slow in wild-type channels in symmetrical  $\text{Na}^+$  solutions after depolarizing steps of sufficient duration (Starkus et al., 1997). Under these conditions, a depolarizing step to positive voltages elicits a current that decays to a steady-state level in  $\sim 60$ – $100$  ms. We attributed this to an accelerated transition into the slow inactivated state. Step repolarizations to  $-100$  mV after shorter first pulse depolarizations resulted in tail currents having two distinct components and increasing the duration of the depolarizing pulse eliminated the fast tail component. More recent data showed that the rising phase and the slow decay of  $\text{Na}^+$  tail currents with the ensuing slowing of charge recovery in both channel types are the result of transitions through two or more inactivated states (Wang et al., 2000; Wang and Fedida, 2001).

We confirmed our earlier observations on wild-type channels in symmetrical  $\text{Na}^+$  solutions (Figs. 5, A and B). When a 15-ms first pulse was applied, the relationship between channel closing and charge recovery was different from that seen in W434F (Figs. 2 B and 5 A). The difference was due to the fast component of the tail current, which meant many channels closing without much charge recovery. However, when the first pulse duration was extended to 1,000 ms and all the channels entered the slow inactivated state, the relationship became linear, as in W434F (Figs. 2 B and 5 B).

In symmetrical  $\text{Tris}^+$  solutions gating charge recovery is also very slow both in the mutant and the wild-type channels (single exponential time constants:  $10.58 \pm 0.61$  ms,  $n = 18$ , and  $13.60 \pm 1.48$  ms,  $n = 21$ , respec-

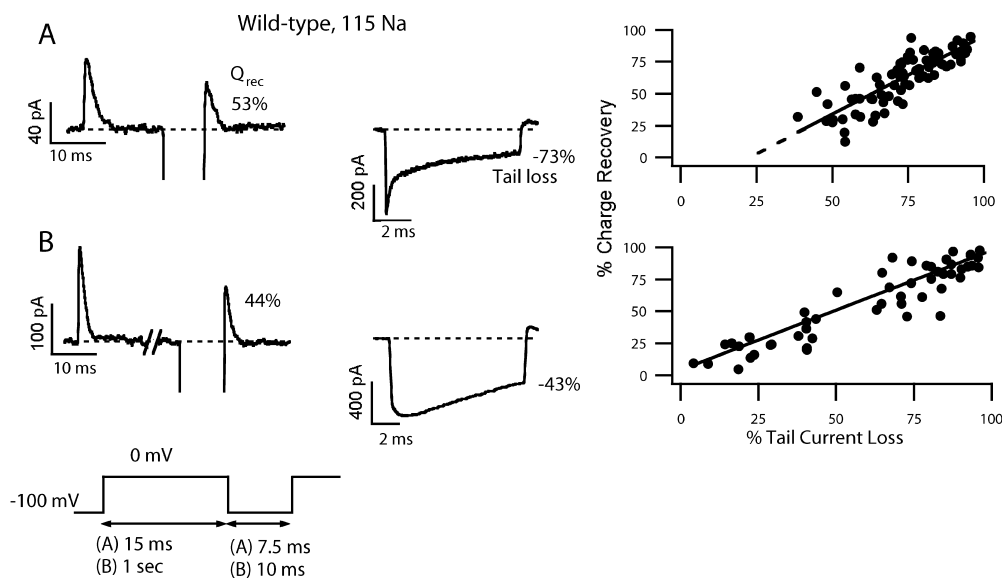


FIGURE 5. The relationship between gating charge recovery and channel closure in the wild-type channel in 115  $\text{Na}^+$  solutions. The figure was prepared as described in the legend to Fig. 2. (A)  $\text{Na}^+$  tail currents have at least two components in the wild-type channel after short ( $<60$ – $100$  ms) first depolarizing pulses. After a 15-ms depolarizing pulse  $\sim 30\%$  of the tail current decays with the fast component (middle). Due to this, charge recovery lags behind channel closing, which is illustrated by the point plot (right,  $n = 14$ ). (B) After a 1,000-ms depolarizing pulse the fast component of the tail current disappears and the relationship be-

tween gating charge recovery and tail current loss becomes 1:1 linear (right,  $n = 13$ ), like it is in the W434F mutant. The data traces shown were obtained from different patches. Percentage values indicate the fraction of recovered gating charge on the left panels and the fraction of tail current amplitude decrease on the middle panels for these recordings.

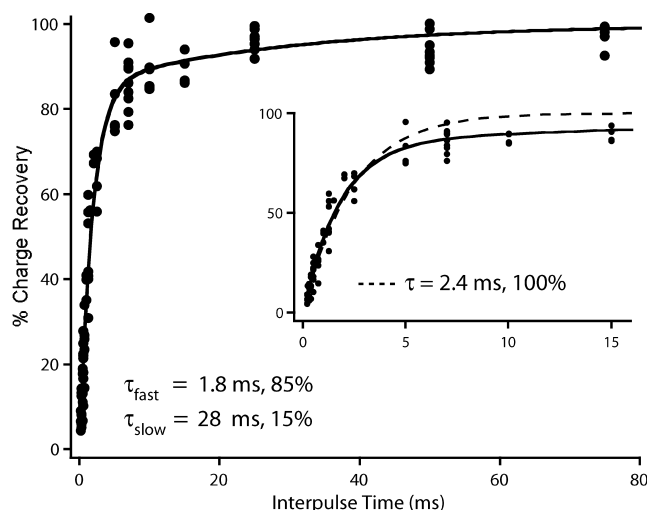


FIGURE 6. The slow component of charge return becomes apparent in scatter plots. The fraction of recovered gating charge is plotted as a function of the interpulse duration used in the double pulse protocol. A single exponential fit to all data points yields a time constant of 2.4 ms, but this function gives a poor fit for interpulse durations over 5 ms (inset, dashed line). A double exponential fit with fast and slow time constants of 1.8 and 28 ms and relative weights of 85 and 15%, respectively, fits the data points well (solid line in both figure and inset). This scatter plot contains data recorded in symmetrical 1 K<sup>+</sup> + 115 Tris<sup>+</sup> solutions from 29 patches containing wild-type channels.

tively, using 15-ms depolarizing pulses), presumably due at least in part to enhanced inactivation induced by the absence of normally permeant ions, as it is the case for Na<sup>+</sup>. This confirms earlier observations that gating charge recovery is slow when no permeating ions (K<sup>+</sup>, Cs<sup>+</sup>, or Rb<sup>+</sup>) are present (Chen et al., 1997; Starkus et al., 1997, 1998; Wang et al., 1999; Loboda et al., 2001).

#### *A Slow Component of Charge Recovery Is Modulated by Cations*

With inactivated states so obviously influencing the rate of charge return in Na<sup>+</sup> solutions, we examined other ionic conditions for the possible involvement of inactivation as well. Although small slow components are difficult to detect in decaying OFF gating currents or from a few data points from single patches, they can be resolved from scatter plots containing data points from a large number of patches. Such a scatter plot is shown on Fig. 6 for the wild-type channel in symmetrical 1 K<sup>+</sup> solutions. The fraction of the ON gating charge that recovered during the repolarizing pulse was determined by integrating the second ON gating current in the double pulse protocol and was plotted as a function of the duration of the repolarizing step. The plot contains data from 29 patches. A single exponential fit to all data points gives an adequate fit for the first 5 ms, but deviates from the data points considerably in the 5–15

ms range (inset, dashed line), and the introduction of a second slow component markedly improves the fit (solid line). For this particular condition, the fast component ( $\tau = 1.8$  ms) comprised 85% of the total amplitude and the slow time constant was 28 ms (15%).

Analysis of other ionic conditions in both channel types revealed a slow component in virtually every case (Fig. 7). The slow time constant ranged from 18 to 30 ms in most cases; however, in some conditions constraining the slow time constant was necessary to get meaningful values. For this reason the slow time constants were not included in Fig. 7.

A pattern that clearly emerges from Fig. 7 is that cations were effective in the prevention of the appearance of the slow component in the following sequence: Cs<sup>+</sup> > Rb<sup>+</sup> > K<sup>+</sup> > Tris<sup>+</sup> > Na<sup>+</sup>. This sequence shows resemblance to the ones found for the slowing of slow inactivation (Fedida et al., 1999), the prevention of the slowing of gating charge return (Wang et al., 1999), and also the affinity for the external lock-in site (Harris et al., 1998), although these studies used NMG<sup>+</sup> instead of Tris<sup>+</sup> as a large nonpermeant cation. As opposed to the sequence found here, Na<sup>+</sup> was more effective than NMG<sup>+</sup> in these studies, which may be due to differences between Tris<sup>+</sup> and NMG<sup>+</sup>. Another possible explanation is that in contrast to our experiments, Na<sup>+</sup> permeation in these other studies was negligible or not present. The second of these studies suggested that the slowing of gating charge return in certain ionic conditions is due to an accelerated rate of inactivation. The external lock-in site is also believed to be involved in the regulation of inactivation (Lopez-Barneo et al., 1993; Baukowitz and Yellen, 1995, 1996; Kiss and Korn, 1998). It is therefore likely that the slow component of charge recovery seen here is the result of slow inactivation, quite possibly regulated by the occupancy of the external lock-in site.

Two more patterns are worth noting from the graph: first, symmetrical reduction of the concentration of Cs<sup>+</sup>, Rb<sup>+</sup>, K<sup>+</sup>, or Na<sup>+</sup> from 115 to 1 mM (substituted by 115 Tris<sup>+</sup>) mostly affected the fast component of charge recovery and had no significant effect on the weight of the components. The overall rates of charge recovery in these conditions based on single exponential time constants were not statistically different ( $P = 0.97$ , ANOVA). Our results confirmed the findings of Wang et al. (1999), which showed that increasing the concentration of Cs<sup>+</sup> in either the internal or the external solution increased the rate of gating charge recovery. Second, the weight of the slow component increased more dramatically upon the removal of permeant ions (Na<sup>+</sup> and Tris<sup>+</sup> conditions) in the wild-type channel than in the mutant. When 1,000-ms long depolarizing pulses were used, not only the weight of the slow component increased in the wild-type channel in



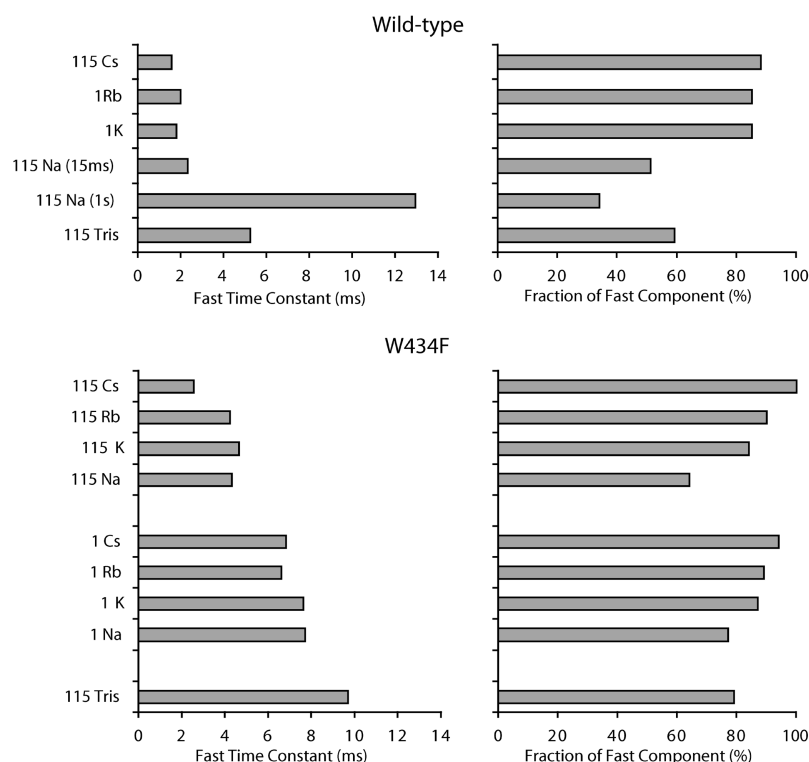


**FIGURE 7.** Fast time constants of charge recovery and their relative weights in wild-type and mutant channels. Data were obtained from double exponential fits to scatter plots in the indicated ionic conditions. Symmetrical solutions were used and the labels indicate the main cation and its concentration in mM in both solutions. When a concentration of 1 mM was used for an ion, it was complemented by 115 mM Tris<sup>+</sup>. For most conditions, the slow time constant fell in the 18–30 ms range. When in some conditions the double exponential fit yielded unreasonably slow time constants, it was constrained within this range to get meaningful values. This did not affect the quality of the fit. For this reason the slow time constants are not shown in the figure. For the wild-type channel, the values in parentheses for the 115 Na<sup>+</sup> condition indicate the duration of the first depolarizing pulse in the double pulse protocol.

Na<sup>+</sup> solutions, but both time constants became much slower (12.9 and 54.4 ms).

#### *The Effects of Ba<sup>2+</sup> on the Rate of Charge Recovery Depend on the Monovalent Cations Present*

By what mechanism do ions modulate the rate of channel closing besides affecting the rate of inactivation? Melishchuk and Armstrong (2001) have found that even small permeant cations must leave the channel cavity before the channel gate can close. The finding that intracellular cations are much more effective at modulating gating charge return in hKv1.5 W472F mutant channels than extracellular cations also supports this model (Wang et al., 1999).

The dwell time of an ion in the cavity is probably determined mostly by its interaction with the cavity wall and with the ion next to it inside the channel pore. The “internal lock-in” effect described by Neyton and Miller (1988a), in which elevated internal K<sup>+</sup> concentrations slowed the inward dissociation of Ba<sup>2+</sup> bound at the deep site of the channel, provides proof for the interaction between ions bound at the deep and internal lock-in sites. Thus, the ion bound at the deep site must produce a knock-off effect on the ion in the cavity, speeding its exit and, as a result, the closing of the gate.

To investigate how this interaction influences channel closing and charge recovery rates, we used the divalent barium ion to amplify these interactions. Ba<sup>2+</sup> is known to block many types of K<sup>+</sup> channels and was shown by X-ray crystallography to bind to the deep K<sup>+</sup>

binding site in KcsA channels (Jiang and MacKinnon, 2000). Other studies have shown that barium can also bind to the external lock-in site, and two Ba<sup>2+</sup> ions can reside within the pore simultaneously (Hurst et al., 1995; Harris et al., 1998). Ba<sup>2+</sup> binding also accelerated OFF gating current kinetics in the W434F mutant (Hurst et al., 1997). We studied the effect of Ba<sup>2+</sup> on the rate of gating charge recovery in the W434F mutant in different ionic conditions.

Fig. 8 A shows that the extent of barium’s effect on accelerating charge recovery was strongly dependent on the cations present in the external and internal solutions. We compared the rates of charge return of inside-out patches in external solutions containing 1.8 mM Ca<sup>2+</sup> with ones in external solutions containing 2 mM Ba<sup>2+</sup>. As earlier, we first used single exponential approximations to make comparisons easier. The effect of replacing Ca<sup>2+</sup> with Ba<sup>2+</sup> in the external solution was weaker in 115 Na<sup>+</sup><sub>o</sub>/115 Na<sup>+</sup><sub>i</sub> solutions (single exponential time constants: Ca<sup>2+</sup>, 8.28 ± 0.82 ms, *n* = 18; Ba<sup>2+</sup>, 4.07 ± 0.41 ms, *n* = 9) than in NFR (115 Na<sup>+</sup> + 2.5 K<sup>+</sup>)<sub>o</sub>/115 K<sup>+</sup><sub>i</sub> solutions (time constants: Ca<sup>2+</sup>, 5.87 ± 0.65 ms, *n* = 8; Ba<sup>2+</sup>, 1.27 ± 0.11 ms, *n* = 5), and no acceleration of gating charge recovery was observed in 115 Tris<sup>+</sup><sub>o</sub>/115 Tris<sup>+</sup><sub>i</sub> solutions (time constants: Ca<sup>2+</sup>, 10.58 ± 0.61 ms, *n* = 18; Ba<sup>2+</sup>, 10.47 ± 0.93 ms, *n* = 6; *P* = 0.93).

The double exponential fit parameters obtained from scatter plots provide a means for a more detailed analysis of barium’s effects (Fig. 8, B and C). Similarly

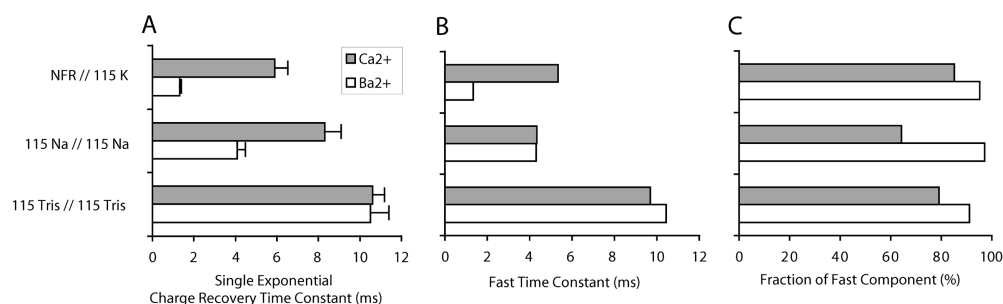


FIGURE 8. The effect of external barium on charge recovery rates in the W434F mutant. (A) The overall charge recovery rates are comparisons based on single exponential fits in external solutions containing 1.8 mM  $\text{Ca}^{2+}$  (dark bars) and external solutions containing 2 mM  $\text{Ba}^{2+}$  (light bars). Labels indicate the composition of the external/internal solutions.

Overall, barium had a stronger effect on the rate of charge return in  $115 \text{ Na}^+ + 2.5 \text{ K}^+_{\text{O}}/115 \text{ K}^+_{\text{I}}$  solutions than in symmetrical  $115 \text{ Na}^+$  solutions, and had no effect in symmetrical  $115 \text{ Tris}^+$  solutions. Bars indicate the mean  $\pm$  SEM of single exponential time constants determined for individual patches. (B and C) Fast time constants of charge recovery and their relative weights obtained from double exponential fits to scatter plots, as described in the legend to Fig. 7. Barium decreased the weight of the slow component in every condition, most notably in  $\text{Na}^+_{\text{O}}/\text{Na}^+_{\text{I}}$ . Barium accelerated the fast component when  $\text{K}^+$  was present, but did not affect it in  $\text{Na}^+$  and  $\text{Tris}^+$  solutions.

to  $\text{Cs}^+$ , the presence of  $\text{Ba}^{2+}$  reduced or almost eliminated the slow component of gating charge return. Since  $\text{Ba}^{2+}$  was applied externally and it does not permeate, this supports the idea that the modulatory site is the external lock-in site rather than a site near the internal end of the pore.

The mechanism by which barium affects charge recovery seems to be different depending on the cations in the solutions. In symmetrical  $\text{Na}^+$  solutions, the acceleration of charge return can be completely ascribed to the elimination of the slow component, whereas the fast component was unaffected. By contrast, in  $\text{NFR}_{\text{O}}/115 \text{ K}^+_{\text{I}}$  solutions, most of the increase in the recovery rate seems to result from the acceleration of the fast component along with a smaller decrease in the weight of the slow component. Although some reduction was present in the slow component in external  $\text{Ba}^{2+}$ , there was no significant overall change in the rate of charge return in symmetrical  $\text{Tris}^+$  solutions.

These differences may be explained by several mechanisms. First, the occupancy of the deep site by  $\text{Ba}^{2+}$  can be very different in these ionic conditions, which in turn can affect barium's interaction with the ion in the cavity. Second, the affinity of the cavity for the different ion species may also vary, producing different exit rates from the cavity. Third, the strength of the interaction between  $\text{Ba}^{2+}$  and the cavity ion may depend on the ion species occupying the cavity. The  $\text{Tris}^+$  ion, for example, may be able to protrude into the cavity and prevent gate closure, but not enter deeply enough to be repelled by  $\text{Ba}^{2+}$ . It may be difficult to distinguish between the two latter possibilities experimentally.

We first addressed the possibility that variations in pore occupancy by  $\text{Ba}^{2+}$  are responsible for the differences. Barium's dissociation constant was found to be in the mM range both in wild-type and W434F mutant channels in solutions containing high concentrations of  $\text{K}^+$  (Hurst et al., 1995, 1997). The experiment shown

in Fig. 9 A demonstrates that barium's affinity for the deep site is much higher in  $\text{K}^+$ -free solutions than in  $\text{K}^+$ -containing solutions. In the figure, the  $\text{Na}^+$  currents from an outside-out patch recorded in  $36 \text{ Na}^+ + 79 \text{ Tris}^+_{\text{O}}/115 \text{ Na}^+_{\text{I}}$  solutions are shown before and after the application of  $1 \mu\text{M}$   $\text{Ba}^{2+}$  in the external solution. Despite the 90 mV driving force (depolarizing pulses to 60 mV and reversal potential of  $-30$  mV), virtually all the current through the channels is blocked by barium. In  $\text{K}^+$ -free solutions,  $\text{Ba}^{2+}$  blocked  $\text{Na}^+$  currents through wild-type channels with similar efficacy. The observed higher affinity is presumably the result of the lack of competition between  $\text{K}^+$  and  $\text{Ba}^{2+}$  ions. Thus, in  $\text{Na}^+$  and  $\text{Tris}^+$  conditions, the occupancy of the deep site by  $\text{Ba}^{2+}$  should be greater, and a stronger effect on the rate of charge recovery would be expected than in  $\text{K}^+$ -containing solutions. Our observations showed just the opposite (Fig. 8), so barium's different affinity for the deep site in  $\text{K}^+$ -containing and  $\text{K}^+$ -free solutions is not a likely explanation for barium's stronger effect in  $\text{K}^+$ -containing solutions.

Since  $\text{Ba}^{2+}$  could block permeation by occupying either the deep or the external lock-in site and  $2 \text{ mM}$   $\text{Ba}^{2+}$  was constantly present in the external solution, the previous experiment does not rule out the possibility that  $\text{Ba}^{2+}$  bound to the deep site dissociates quickly to the inside. This may be even more likely in an internal  $\text{Tris}^+$  solution. To test this, we measured how quickly bound  $\text{Ba}^{2+}$  dissociated from the channels in an outside-out patch. In  $115 \text{ Na}^+_{\text{O}}/115 \text{ Tris}^+_{\text{I}}$  solutions, a step pulse to 0 mV followed by a return to  $-100$  mV evoked a small inward  $\text{Na}^+$  current followed by a large  $\text{Na}^+$  tail current (Fig. 9 B, trace 1). The external solution was then switched to  $115 \text{ Tris}^+ + 2 \text{ Ba}^{2+}$  (trace 2) for 18 s then switched back to  $115 \text{ Na}^+$  again to assess the extent of block. The first trace recorded 8 s after the switch showed very little tail current (trace 3), indicating that most of the channels were still blocked by  $\text{Ba}^{2+}$ . Further

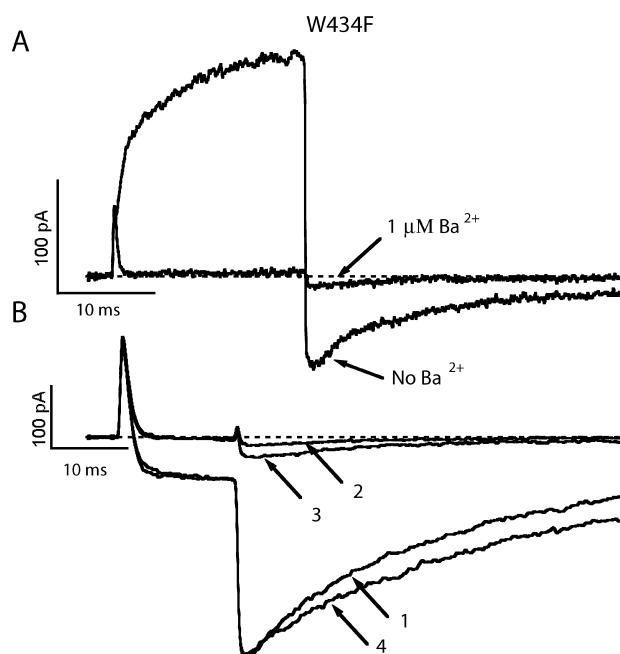


**FIGURE 9.** High affinity block of W434F channels by barium in  $\text{Na}^+$  and  $\text{Tris}^+$  solutions. (A) Micromolar concentration of barium blocks W434F channels in  $\text{K}^+$ -free solutions. Depolarizing steps of 20 ms duration to 60 mV were applied every second from a holding potential of  $-100$  mV. Currents were recorded from an outside-out patch containing W434F channels. The external solution contained (in mM) 36  $\text{Na}^+$  + 79  $\text{Tris}^+$ , and the internal solution was 115  $\text{Na}^+$ , yielding a reversal potential of about  $-30$  mV. Switching to an external solution containing  $1 \mu\text{M Ba}^{2+}$  resulted in an almost complete block of both the outward current and the inward tail current in five pulses. (B) Inward dissociation of  $\text{Ba}^{2+}$  is slow in a  $\text{Tris}^+$  internal solution. Recordings are from an outside-out patch containing W434F channels. The pipette solution (internal solution) contained 115  $\text{Tris}^+$ . The external solution originally was 115  $\text{Na}^+$ . A step pulse to 0 mV for 15 ms followed by a return to  $-100$  mV evoked a small inward  $\text{Na}^+$  current followed by a large  $\text{Na}^+$  tail current (trace 1). The external solution was then switched to 115  $\text{Tris}^+$  +  $2 \text{Ba}^{2+}$ , which abolished all ionic currents, leaving only the gating currents (trace 2). After switching back to 115  $\text{Na}^+$  again, the first trace recorded 8 s after the switch showed very little tail current (trace 3), indicating that most of the channels were still blocked by  $\text{Ba}^{2+}$ . Further washing resulted in the full recovery of the  $\text{Na}^+$  current (trace 4) with a time constant of 38 s.

washing resulted in the full recovery of the  $\text{Na}^+$  current with a time constant of 38 s. Thus, fast inward dissociation of  $\text{Ba}^{2+}$  in  $\text{Tris}^+$  solutions is unlikely.

#### *Barium Can Affect the Rate of Charge Recovery both from Deep and External Lock-in Sites*

The experiment in Fig. 10 addresses the question of whether barium at the external lock-in or the deep site is responsible for the changes in charge recovery rate. The external lock-in site probably equilibrates very quickly with the external solution, whereas association to and dissociation from the deep site is expected to be slower. The traces shown were recorded in symmetrical

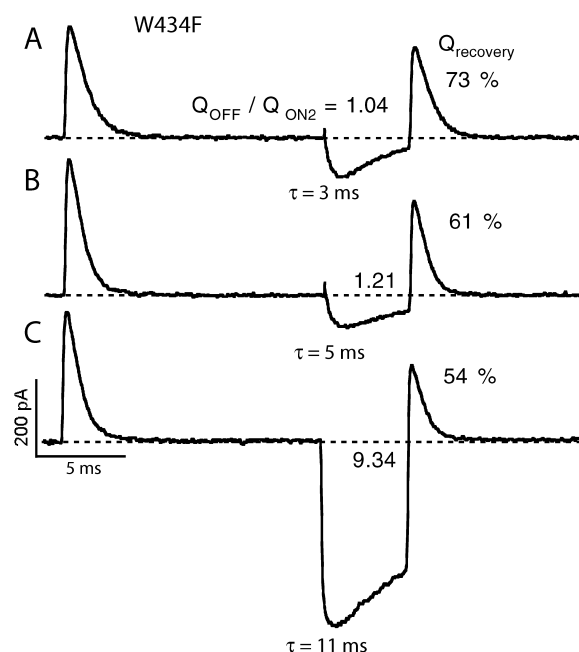


**FIGURE 10.** Barium affects the rate of charge recovery from both the deep and the external lock-in sites. The traces shown were recorded in symmetrical 115  $\text{Na}^+$  solutions from an outside-out patch containing W434F channels. From a holding potential of  $-100$  mV the voltage was stepped to 0 mV for 15 ms, then returned to  $-100$  mV for 5 ms, and then returned again to 0 mV. (A) In the presence of 10 mM external  $\text{Ba}^{2+}$  charge recovers quickly, which is indicated by the fast decay of the OFF gating current ( $\tau = 3$  ms) and the high fraction of recovered charge in the second ON pulse (73%). The  $Q_{\text{OFF}}/Q_{\text{ON2}}$  ratio, which is the ratio of integrated charge in the OFF gating current + tail current to that in the ON gating current in the second pulse, shows that there is no inward  $\text{Na}^+$  permeation during the repolarizing pulse. (B) 2 s after switching to  $\text{Ba}^{2+}$ -free solution the  $Q_{\text{OFF}}/Q_{\text{ON2}}$  ratio is still close to unity, signaling negligible permeation, but there is a significant slowing in the OFF gating current decay ( $\tau = 5$  ms), which is also reflected in the lower fraction of recovered charge in the second ON gating pulse (61%). This suggests that  $\text{Ba}^{2+}$  has left from the external lock-in site, but not the deep site. (C) 46 s after the switch a large  $\text{Na}^+$  tail current is seen during the repolarizing pulse ( $Q_{\text{OFF}}/Q_{\text{ON2}} = 9.34$ ), signaling  $\text{Ba}^{2+}$  exit from the deep site, and further slowing of the charge recovery rate is observed ( $\tau = 11$  ms,  $Q_{\text{rec}} = 54\%$ ).

115  $\text{Na}^+$  solutions from an outside-out patch containing W434F channels. The trace on Fig. 10 A was recorded in the presence of 10 mM  $\text{Ba}^{2+}$  in the external solution, the one on Fig. 10 B 2 s after switching to  $\text{Ba}^{2+}$ -free solution, and the one on Fig. 10 C 46 s later, still in  $\text{Ba}^{2+}$ -free  $\text{Na}^+$  solution. The percentage values represent the amount of gating charge that recovered during the 5 ms repolarizing pulse to  $-100$  mV, whereas the tau values are the single exponential time constants of the OFF gating current/tail current decay. The  $Q_{\text{OFF}}/Q_{\text{ON2}}$  ratio is the ratio of integrated charge in the OFF gating current + tail current to that in the ON gating current in the second pulse. This ratio should be one if there was only OFF gating current and no ionic current during

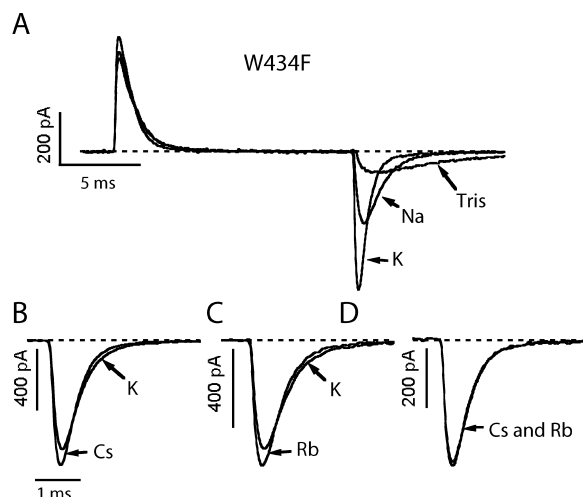


FIGURE 11. The effect of internal cations on OFF gating current kinetics. Inside-out patches containing W434F channels were exposed to internal solutions containing 115 mM Tris<sup>+</sup>, Na<sup>+</sup>, K<sup>+</sup>, Rb<sup>+</sup>, or Cs<sup>+</sup>, whereas the external solution was NFR + 5 mM Ba<sup>2+</sup>. Under these conditions, the occupancy of the deep site by Ba<sup>2+</sup> is high and barium's interaction with the ion in the cavity will determine the rate of channel closing and OFF gating current decay. Channels were opened by a 15-ms pulse to 0 mV then the voltage was returned to the holding potential of -100 mV eliciting the OFF gating currents. Each part of the figure shows results from a different patch. (A) OFF gating current decay was the slowest with Tris<sup>+</sup> as the internal cation ( $\tau = 5.62$  ms in this patch), was faster in Na<sup>+</sup> ( $\tau = 1.25$  ms), and still faster in K<sup>+</sup> ( $\tau = 615$   $\mu$ s). (B–D) Differences in OFF gating kinetics were small or negligible when the internal solution was switched between any two of K<sup>+</sup>, Cs<sup>+</sup>, or Rb<sup>+</sup>. B, switch between Cs<sup>+</sup> ( $\tau = 394$   $\mu$ s) and K<sup>+</sup> (465  $\mu$ s); C, between Rb<sup>+</sup> (477  $\mu$ s) and K<sup>+</sup> (564  $\mu$ s); and D, between Cs<sup>+</sup> (434  $\mu$ s) and Rb<sup>+</sup> (407  $\mu$ s).

the repolarizing pulse. What the figure clearly illustrates is that right after the switch to 0 Ba<sup>2+</sup>, there is virtually no increase in the charge ratio (negligible Na<sup>+</sup> permeation), indicating that Ba<sup>2+</sup> is still in the pore in almost every channel, but there is a marked slowing in the OFF gating current decay, which is also reflected in the lower fraction of recovered charge in the second ON gating pulse. Further washing resulted in the recovery of the Na<sup>+</sup> tail current, which is indicated by a  $Q_{\text{OFF}}/Q_{\text{ON2}}$  ratio of 9.34, and further slowing of the charge recovery rate (slower decay time constant and less charge in the second ON gating pulse).

Our interpretation of this result is that at the time of the first pulse after the start of the washing, the Ba<sup>2+</sup> ions have already dissociated from the external lock-in site, but the lack of any tail current suggests that the deep site of virtually every channel still holds a Ba<sup>2+</sup> ion. The slow relief from block signals the rate of Ba<sup>2+</sup> dissociation from the deep site. Thus, it appears that occupancy of both the deep and external lock-in sites by Ba<sup>2+</sup> affect the rate of charge recovery.

Fig. 8 B indicates that barium accelerated the fast component of charge return in the presence of K<sup>+</sup>, but

not in the presence of Na<sup>+</sup> or Tris<sup>+</sup>. To further investigate this phenomenon, we compared OFF gating currents in the same inside-out patch keeping the external solution constant (NFR + 5 mM Ba<sup>2+</sup>) and switching between internal solutions containing 115 mM K<sup>+</sup>, Cs<sup>+</sup>, Rb<sup>+</sup>, Na<sup>+</sup>, or Tris<sup>+</sup> (Fig. 11). Under the conditions used, a high occupancy of the deep site by Ba<sup>2+</sup> is expected. Therefore, OFF gating current kinetics in this case only depend on the ion in the cavity. In the experiment we measured the decay rates of OFF gating currents upon return to -100 mV after a 15-ms step to 0 mV. OFF gating currents had similar fast kinetics with Cs<sup>+</sup>, Rb<sup>+</sup>, or K<sup>+</sup> as the internal cation. The sequence for the speed of OFF gating current kinetics was Cs<sup>+</sup>  $\approx$  Rb<sup>+</sup> > K<sup>+</sup>, but differences among these internal ions were marginal. OFF gating kinetics became slower in a 115 mM Na<sup>+</sup> internal solution, and yet much slower when Na<sup>+</sup> was replaced by Tris<sup>+</sup>. These results indicate that the exit rates of these internal cations from the cavity can be very different, even when the deep site is occupied by the same ion.

#### Barium Can Slow Charge Return in the Wild-type Channel

An unexpected result is shown in Fig. 12. Although Ba<sup>2+</sup> accelerated the rate of charge recovery in most cases in the mutant channel, charge recovery was slower in the wild-type channel in symmetrical 115 Tris<sup>+</sup> + 1K<sup>+</sup> solutions in the presence of 2 mM external Ba<sup>2+</sup> than in its absence (single exponential time constants:  $2.80 \pm 0.23$  ms without Ba<sup>2+</sup>,  $n = 29$ ;  $4.73 \pm 0.35$  ms with Ba<sup>2+</sup>,  $n = 7$ ;  $P < 5.6 \times 10^{-3}$ ). In the figure, two traces recorded from an inside-out patch show as the

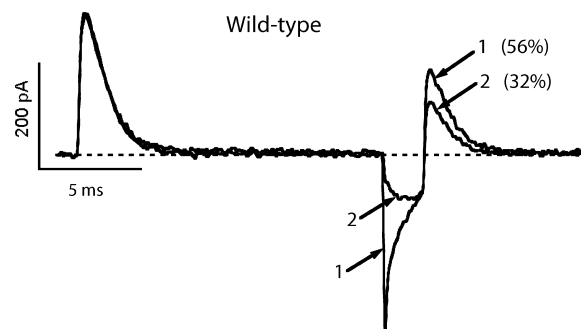


FIGURE 12. Block of K<sup>+</sup> conduction in the wild-type channel by external Ba<sup>2+</sup> slows the rate of charge recovery. The traces were recorded from an inside-out patch in symmetrical 1 K<sup>+</sup> + 115 Tris<sup>+</sup> solutions with the addition of 2 mM Ba<sup>2+</sup> in the pipette. From a holding potential of -100 mV a pair of pulses to 0 mV was applied, separated by 2 ms at -100 mV. Trace 1, recorded first, shows some fast inward K<sup>+</sup> tail current and a greater amount of charge recovered in the second pulse (56%). As barium in the pipette solution diffuses into the channels, it blocks the potassium tail current, leaving only the OFF gating current (trace 2). Along with the disappearance of the tail current, a clear slowing of the charge recovery rate is visible in the second ON gating current (32%).

barium in the pipette solution diffuses into the channels and blocks the potassium tail current, leaving only the OFF gating current. Along with the disappearance of the tail current a clear slowing of the charge recovery rate is visible in the second ON gating current. Double exponential fits from the scatter plots revealed that the slowing originates from the fast component, and the weight of the slow component was decreased by  $\text{Ba}^{2+}$  as in all other cases (without  $\text{Ba}^{2+}$ :  $\tau_{\text{fast}} = 1.79$  ms,  $A_{\text{fast}} = 85\%$ ; with  $\text{Ba}^{2+}$ :  $\tau_{\text{fast}} = 4.03$  ms,  $A_{\text{fast}} = 89\%$ ).

## DISCUSSION

In the present work we have studied the relationship between the rate of the closing of the internal gate upon repolarization and the rate of gating charge return in fast inactivation removed wild-type and W434F mutant *Shaker* channels. We have also examined how various cation species affect these rates and attempted to elucidate the mechanisms that are responsible for these effects.

As our results show, conclusions drawn about these rates from observations on nonconducting mutants or conducting channels in solutions free of permeating ions may not apply to conducting channels in solutions containing permeating ions, and thus such observations must be interpreted with care.

It has been known for a long time that the type of ion permeating through the wild-type channel influences the rate at which the channel closes. The different tail current decay rates obtained in this study confirm this observation (Fig. 3 B). Yet, despite the variations in channel closing rate, the rate of gating charge recovery is not significantly different in these ionic conditions (Fig. 3 A). Since, during deactivation, channel closure precedes the transitions associated with most of the charge movement, this is only possible if the first closing step is considerably faster than the subsequent charge carrying steps. Comparison of the tail current and charge recovery time constants reveals that channel closing is in fact 2–3 times faster than charge return in symmetrical 1  $\text{K}^+$ , 1  $\text{Rb}^+$ , and 115  $\text{Cs}^+$  conditions (also Fig. 1 C). The plot illustrating the relationship between the two quantities clearly proves this point (Fig. 2 A).

The concentration of cations in the external and internal solutions for the wild-type channel was adjusted based on their permeabilities. When higher concentrations of  $\text{K}^+$  or  $\text{Rb}^+$  were used, the sections of the current traces recorded during the two pulses to 0 mV were usually contaminated by some ionic current preventing accurate determination of the gating charge. Furthermore, large ionic tail currents in these conditions caused local accumulation of cations, leading to changes in reversal potential and ultimately ionic current contamination in the gating currents. On the other hand, low concentrations of  $\text{Cs}^+$  did not produce large

enough tail currents for precise measurements of decay rates. In the mutant channel, the lack of permeation reduces the access of ions to binding sites inside the pore, so the application of high concentrations of these ions (115 mM) was necessary to see an effect characteristic of that particular ion rather than the substitute ion  $\text{Tris}^+$ .

In the nonconducting W434F mutant, various ionic conditions produced different rates of charge recovery (Fig. 3 C) and these rates were slower than those of the wild-type channel (Fig. 3 A). Evidence shows that these differences only appear if the channels are first opened by strong enough depolarization (Perozo et al., 1993; Wang et al., 1999). It has also been suggested that the closing of the internal gate is prevented by even a small permeant ion in the cavity (Melishchuk and Armstrong, 2001). All these results imply that in the mutant channel gate, closure becomes slow enough to be rate-limiting in the recovery of gating charge.

Although charge recovery was significantly faster in 115  $\text{K}^+_{\text{O}}/115 \text{K}^+_{\text{I}}$  than 115  $\text{Tris}^+_{\text{O}}/115 \text{Tris}^+_{\text{I}}$  solutions in the mutant channel (Fig. 7), it became slower when  $\text{K}^+$  was present only externally. In this 115  $\text{K}^+_{\text{O}}/115 \text{Tris}^+_{\text{I}}$  condition a very slowly decaying  $\text{K}^+$  tail current was detectable (Fig. 4 A), whereas there was no tail current in 115  $\text{K}^+_{\text{O}}/115 \text{K}^+_{\text{I}}$  solutions. Since the rates of charge recovery and channel closing were the same in this condition (Fig. 4 E), this means that the return of gating charge was much slower when  $\text{K}^+$  permeation was present. Also, charge recovery in the nonconducting Kv1.5-W472F (analogue of W434F) was slower in  $\text{NMG}^+_{\text{O}}/\text{NMG}^+_{\text{I}}$  solutions than in  $\text{Rb}^+_{\text{O}}/\text{NMG}^+_{\text{I}}$  solutions, where  $\text{Rb}^+$  showed no signs of permeation (Wang et al., 1999). This is in contrast to our finding that current decay was slightly faster in  $\text{Tris}^+_{\text{O}}/\text{Tris}^+_{\text{I}}$  than in  $\text{Rb}^+_{\text{O}}/\text{Tris}^+_{\text{I}}$  solutions, where we observed some  $\text{Rb}^+$  permeation (Fig. 4 B). Of course, the difference may arise from the use of different solutions and different channel types. However, the results of that study and the ones shown here are otherwise very similar, which leads us to believe that the difference stems from the presence or absence of ion permeation. Thus, ion permeation appears to be a strong determinant of channel closing rate in the mutant channel too, similarly to the slowing of tail currents in wild-type channels induced by the raising of external permeant ion concentration and the concomitant increase in ion flux rate.

The nonconducting W434F channel demonstrates a strict linear relationship between channel closing and gating charge return in symmetrical  $\text{Na}^+$  conditions (Fig. 2 B). However, this does not necessarily reflect slow channel closing. There is now a line of evidence for the involvement of inactivated states in the slow channel closing and charge return in wild-type and W434F channels in  $\text{Na}^+$  solutions (Starkus et al., 1997, 1998; Wang et al., 2000; Loboda et al., 2001; Wang and Fedida, 2001).

Closer examination of the time dependence of gating charge return revealed the existence of a slow component in almost every ionic condition in both channel types, suggesting at least partial role of inactivation in determining the charge recovery rate. The occupancy of the external lock-in site is thought to control the rate of slow inactivation (Lopez-Barneo et al., 1993; Baukowitz and Yellen, 1995, 1996; Kiss and Korn, 1998), and some of our data are consistent with its role in influencing the rate of charge return via the regulation of inactivation. For example, ions were effective at reducing the weight of the slow component in the sequence of their affinities for the external lock-in site (Harris et al., 1998). Also, 1 mM of  $\text{Cs}^+$ ,  $\text{Rb}^+$ , or  $\text{K}^+$  was almost as effective at reducing the weight of the slow component as 115 mM, suggesting that the modulatory site has a high affinity for these ions, similarly to the external lock-in site (Neyton and Miller, 1988b; Harris et al., 1998; Kiss and Korn, 1998). Moreover, externally applied  $\text{Ba}^{2+}$  was very effective at eliminating the slow component, which again places the modulatory site near the external end of the pore rather than the internal. Changes in the rate of charge return during the washout of  $\text{Ba}^{2+}$  from the mutant channel in  $\text{Na}^+$  solutions indicated the involvement of both the deep and the external lock-in sites in the modulation (Fig. 10). Since practically all of the accelerating effect of  $\text{Ba}^{2+}$  can be attributed to the elimination of the slow component in  $\text{Na}^+_{\text{O}}/\text{Na}^+_{\text{I}}$ , it leads us to conclude that occupancy of the deep site also regulates the transition into an inactivated state, at least in these solutions.

The question now arises: the effect of which inactivated state(s) do we see in the rate of charge return? Traditionally, the slow decay of the ionic current through fast-inactivation-removed channels was referred to as C-type inactivation. More recently, C-type inactivation was redefined to mean the shift of the charge-voltage ( $Q$ - $V$ ) relationship in response to depolarizations lasting from many seconds to minutes, which causes the slow recovery of gating charge (Chen et al., 1997; Olcese et al., 1997; Loots and Isacoff, 1998). By P-inactivation one usually means a perturbation of the selectivity filter, which prevents further permeation of  $\text{K}^+$ , but allows the permeation of  $\text{Na}^+$  without the  $Q$ - $V$  shift associated with C-inactivation. The W434F mutant is believed to permanently reside in this P-state, but is able to undergo normal closed/open transitions (Perozo et al., 1993; Olcese et al., 1997; Yang et al., 1997; Loots and Isacoff, 1998). Sodium tail currents through the mutant channel exhibit a slow rising phase even after brief depolarizing pulses (Fig. 2 B). This is the result of the transition through a state of higher  $\text{Na}^+$  conductance during the recovery from an inactivated state of lower  $\text{Na}^+$  conductance (Wang et al., 2000). However, this mutant is known to be more

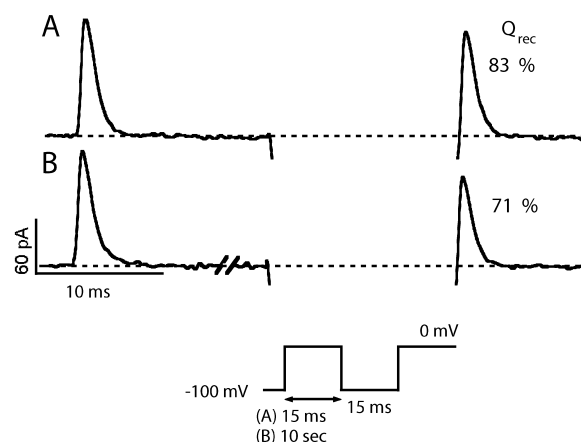


FIGURE 13. W434F channels are slow to enter the C-inactivated state. Traces were recorded in symmetrical 115  $\text{Na}^+$  solutions from an inside-out patch containing W434F channels. The standard double pulse protocol was used with (A) a 15-ms and (B) a 10-s first pulse duration. Despite the dramatic increase in the duration of the first pulse, little slowing in charge recovery is seen (15 ms first pulse: 83%, 10 s first pulse: 71%). The interpulse duration was 15 ms. The large  $\text{Na}^+$  tail currents were omitted from the figure for clarity.

reluctant to enter the C-inactivated state than the wild-type channel. This is manifested in a faster recovery of the ionic current, structural changes monitored by fluorescence signals after long periods at depolarized voltages (Loots and Isacoff, 1998), and a considerably smaller shift of the  $Q$ - $V$  curve than in the wild-type channel (Olcese et al., 1997). This is also seen in the marked slowing of both time constants of recovery and the increased weight of the slow component in the wild-type channel when the duration of the first depolarizing pulse was extended from 15 to 1,000 ms (Fig. 7; 15 ms:  $\tau_{\text{fast}} = 2.3$  ms,  $\tau_{\text{slow}} = 21.4$  ms,  $A_{\text{slow}} = 49\%$ ; 1000 ms:  $\tau_{\text{fast}} = 12.9$  ms,  $\tau_{\text{slow}} = 54.4$  ms,  $A_{\text{slow}} = 66\%$ ). By contrast, drastically extending the duration of the first pulse had little effect on the recovery rate in W434F (Fig. 13), suggesting that entry into the C-inactivated state is much slower than in the wild-type channel. It is therefore not clear what inactivated state the channels are recovering from during the rising phase of the tail current. It is conceivable that an inactivated state exists between the open and C-inactivated states that is reached by a large fraction of channels, yet the transition into which has no significant effect on the rate of charge recovery. Further transition of some channels into the C-state would then cause the  $Q$ - $V$  shift, and the slow component of the charge recovery.

Recent work has shown that closing of the gate can only proceed after the exit of any ion from the internal channel cavity (Melishchuk and Armstrong, 2001). Thus, the fraction of time when the cavity is vacant will determine the rate of channel closure, if the channel is not inactivated. The fraction of vacant periods depends

on the dwell time of the ion in the cavity and the magnitude of permeation that supplies the ions for replacing the ones leaving the cavity. The most obvious factors influencing the dwell time are the membrane potential, the interaction of the ion with another ion next to it inside the channel pore, and its interaction with the cavity wall. We have used  $-100$  mV in all our experiments to measure the rates of channel closing and charge return, so any observed differences must be due to the two latter factors.

To clarify where the differences in the rate of gate closure in various ionic conditions stem from we used  $\text{Ba}^{2+}$  to fill the deep site of the mutant channels. Acceleration of OFF gating current kinetics in W434F mutant channels by barium has been reported by Hurst et al. (1997). This phenomenon is probably at least in part due to the knock-off effect on the ion in the cavity by the ion at the deep site being amplified by the double charge of barium occupying the deep site instead of a monovalent cation.

The addition of 2 mM barium to the external solution considerably accelerated the rate of charge recovery in  $\text{NFR}_\text{O}/\text{K}^+_1$  solutions, had a much weaker effect in  $\text{Na}^+_0/\text{Na}^+_1$  solutions, and had no effect in  $\text{Tris}^+_0/\text{Tris}^+_1$  solutions. As mentioned earlier, these differences may arise from the varying degree of occupancy of the deep site by  $\text{Ba}^{2+}$ . We ruled out this possibility by demonstrating that the channel has a significantly higher affinity for  $\text{Ba}^{2+}$  in  $\text{Na}^+$  conditions than was reported for  $\text{K}^+$ -containing solutions. We believe that at 2 mM external  $\text{Ba}^{2+}$  concentration the deep site in the W434F mutant has a very high occupancy by  $\text{Ba}^{2+}$  for several reasons. We have shown that  $\text{Ba}^{2+}$  dissociation is very slow in  $\text{Na}^+_0/\text{Na}^+_1$  solutions (Fig. 10), and also very slow in  $\text{Na}^+_0/\text{Tris}^+_1$  solutions (Fig. 9 B). Since inward dissociation of  $\text{Ba}^{2+}$  is likely to be even slower with high concentrations of  $\text{K}^+$ ,  $\text{Cs}^+$ , or  $\text{Rb}^+$  in the internal solution (Neyton and Miller, 1988a), significant inward dissociation of barium from the deep site can be ruled out in all of these ionic conditions. Various studies show that low millimolar concentrations of external  $\text{K}^+$  very effectively prevent outward dissociation of bound  $\text{Ba}^{2+}$ , and 2 mM  $\text{Ba}^{2+}$  present in the external solution is even more effective (Neyton and Miller, 1988b; Harris et al., 1998). Thus, significant outward dissociation is also unlikely. Moreover, the study by Hurst et al. (1997) found that the actions of barium on the gating charge movement of W434F *Shaker* channels were dose-dependent with  $\text{EC}_{50} \approx 0.2$  mM and saturated at  $\sim 2$  mM.

We have also shown here that barium's effect in  $\text{Na}^+$  solutions can be fully explained by the elimination of the slow component of charge recovery without any effect on the fast component. Barium also had no effect on the fast component of recovery in  $\text{Tris}^+$  solutions, whereas it significantly accelerated the fast component

when there was 115 mM  $\text{K}^+$  in the internal solution (Fig. 8 B). The effects on the fast component of charge return seem to originate from the ion in the cavity and its interaction with the ion at the deep site. Barium appears to be able to interact strongly with a  $\text{K}^+$  ion in the cavity but not with a  $\text{Tris}^+$  or  $\text{Na}^+$  ion. This idea is supported by the results shown in Fig. 11, in which charge recovery was much slower in  $\text{Tris}^+$  and  $\text{Na}^+$  internal solutions than in  $\text{Cs}^+$ ,  $\text{Rb}^+$ , or  $\text{K}^+$  internal solutions. Being a bulky ion,  $\text{Tris}^+$  probably protrudes into the cavity deeply enough to prevent the closing of the gate, but not deeply enough to interact with  $\text{Ba}^{2+}$  at the deep site. The smaller size of  $\text{Na}^+$  compared with the other ions may explain its lack of interaction with  $\text{Ba}^{2+}$ . The cavity may accommodate more water molecules with an  $\text{Na}^+$  inside, which would screen its charge more than for a larger ion, which would then weaken its electrostatic interaction with  $\text{Ba}^{2+}$ . Alternatively, a stronger interaction of  $\text{Na}^+$  with the cavity wall is also possible.

If  $\text{Tris}^+$  is slow to leave the cavity, the slowing of the fast components of charge recovery is an expected consequence of symmetrical reduction of  $\text{K}^+$ ,  $\text{Cs}^+$ , and  $\text{Rb}^+$  from 115 to 1 mM.

Based on the observations shown in Fig. 11,  $\text{Cs}^+$  left the cavity at about the same rate as  $\text{Rb}^+$  and barely faster than  $\text{K}^+$  when  $\text{Ba}^{2+}$  occupied the deep site. These small differences cannot account for the differences seen in the fast components of charge return in symmetrical 115 mM solutions of these ions. We hypothesize that the occupancy of the deep site is higher in symmetrical 115  $\text{Cs}^+$  than in symmetrical 115  $\text{K}^+$ , which means a higher average interaction energy with the ion in the cavity that would accelerate its exit. The interaction between a pair of  $\text{Cs}^+$  ions may also be stronger than between a pair of  $\text{K}^+$  ions due to structural differences inside the pore that could modify local dielectric constants. Thus, the dwell time of these ions at the deep site probably follows the sequence:  $\text{Cs}^+ > \text{Rb}^+ > \text{K}^+$  (which is supported by their relative permeabilities), and this sequence is reversed for the dwell time in the cavity. These two effects combined may explain the differences in the fast components of charge return.

In the wild-type channel, in which channel closing is not rate-limiting, the fast component of recovery is slightly faster in  $\text{Cs}^+$  than in  $\text{K}^+$  (1.54 and 1.79 ms, respectively). Additionally, the fast component was even faster in the mutant channel in  $\text{NFR} + 2 \text{ Ba}^{2+}_0/115 \text{ K}^+_1$  solutions ( $\tau = 1.26$  ms). Since these values come from individual double exponential fits, and the differences are small, their statistical value is low. Nevertheless, they imply the existence of a weak effect on the transitions between closed states. Thus, based on our data, some direct electrostatic interaction of the ions in the pore with the mobile gating charges of the protein

is also likely. Such direct action by  $\text{Ba}^{2+}$  was proposed by Hurst et al. (1997).

It has been proposed that in Kv1.5 channels a site located inside the pore and more accessible from the internal solution is the dominant regulator of inactivation (Fedida et al., 1999), and that this may be the same site regulating the rate of charge return by regulating inactivation in the nonconducting mutant (Wang et al., 1999). This site might be the deep or the cavity site. The fact that charge recovery became slower in the wild-type channel when  $\text{K}^+$  permeation was blocked by  $\text{Ba}^{2+}$  appears to support this hypothesis. One could argue that the block of ion permeation through the pore reduces the occupancy of the cavity site, which then speeds the transition into an inactivated state, from which recovery is slow.

However, the fact that charge recovery is much slower in the mutant channel when an inward  $\text{K}^+$  tail current is flowing through the channel than when there is no permeation in  $\text{Tris}^+_{\text{O}}/\text{Tris}^+_{\text{I}}$  solutions contradicts this hypothesis. Obviously, based on this model, with  $\text{K}^+$  ions in the pore one would expect more prevention of inactivation and therefore faster charge recovery than without permeation. Even during the depolarizing pulse to 0 mV there is a small inward current, which should be enough to replace  $\text{Tris}^+$  in the cavity by  $\text{K}^+$  and thus prevent inactivation.

Instead, we believe that the slowing of charge recovery in the wild-type channel when blocked by barium is simply the result of mostly  $\text{Tris}^+$  occupying the cavity instead of  $\text{K}^+$ , and the longer dwell time of  $\text{Tris}^+$  compared with  $\text{K}^+$ .

#### *A Model of the Effects of Cations on the Rate of Charge Recovery*

We attempted to assemble a model that would qualitatively account for most of the ionic effects on the rate of gating charge recovery in both channel types. Due to the apparent complexity of the regulating mechanisms and the many conditions we examined, we did not intend to reproduce all results quantitatively.

For modeling transitions in both channel types we added a series of C-inactivated states ( $\text{I}_{\text{Ci}}$ ) to the closed (C) and open states (O), since the presence of a slow component was apparent in most ionic conditions (Fig. 14). Extending the duration of the depolarizing pulse causes a continuous slow shift of the Q-V function, which is better represented by transitions into a series of deeper C-inactivated states, the recovery from which is progressively slower, than just one C-inactivated state. To account for the rising phase of  $\text{Na}^+$  tail currents we included an inactivated state ( $\text{I}_0$ ) that is reached by a large fraction of channels in  $\text{Na}^+$  conditions, but one that has no significant shift in the Q-V relationship compared with the open state. Based on the scheme of

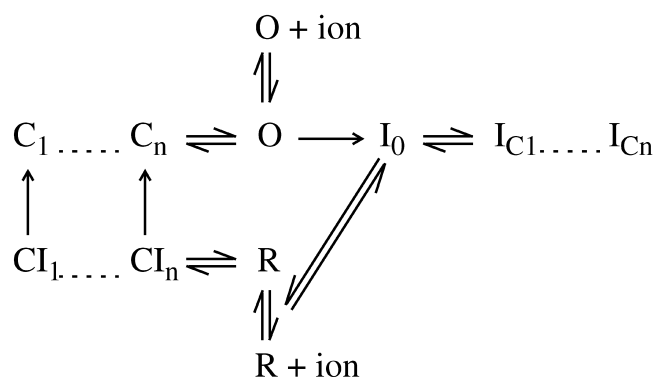


FIGURE 14. A model to account for the effects of cations on the gating charge recovery in wild-type and W434F channels. In accordance with current models of activation, the channel has to traverse a series of closed states before opening. The transition into  $\text{I}_0$  is modulated by cations from the external lock-in site, being the fastest in  $\text{Na}^+$  and  $\text{Tris}^+$ . A fraction of the channels move on to C-inactivated states that are associated with the shift of the Q-V function. Reaching deeper C-states results in progressively slower charge recovery. Upon repolarization, wild-type channels close quickly from the O state, but the ones recovering from  $\text{I}_0$  close more slowly into closed-inactivated states through  $\text{R} \rightarrow \text{CI}_n$  due to the slower intrinsic rate of this transition. In the mutant channel, the closing rate of the gate is the same in both branches, and is similar to the closing rate of the wild-type in the lower branch. Closing of the gate in both the top and bottom branches is prevented by ions occupying the cavity, which is represented by the O+ion and R+ion states. Inward ion permeation or internal  $\text{Tris}^+$  causes a higher population of the O+ion and R+ion states and thus hinders channel closing. The slow recovery from the C-inactivated states generates the slow component of charge recovery. The fast  $\text{I}_0 \rightarrow \text{R}$  transition along with the higher  $\text{Na}^+$  conductance of the R state is responsible for the rising phase of  $\text{Na}^+$  tail currents in both channel types.

Wang et al. (2000), we also added another state (R) in the recovery from inactivation pathway that has a higher  $\text{Na}^+$  conductance than the inactivated states (Wang and Fedida, 2001). In the scheme, all the inactivated states ( $\text{I}_0$  and  $\text{I}_{\text{Ci}}$ ) are assumed to have the same  $\text{Na}^+$  conductance. In the wild-type channel, the open state has a high  $\text{Na}^+$  conductance, similar to R, which has about twice the conductance of the inactivated states. In the mutant, the conductance of the open state is only  $\sim 20\%$  of the conductance of R. Thus, the conductance ratios are: wild-type,  $\text{G}(\text{O}):\text{G}(\text{I}_0, \text{I}_{\text{Ci}}):\text{G}(\text{R}) = 1:0.5:1$ ; W434F,  $\text{G}(\text{O}):\text{G}(\text{I}_0, \text{I}_{\text{Ci}}):\text{G}(\text{R}) = 0.2:0.5:1$ . These conductance ratios and a fast opening transition followed by a slower  $\text{O} \rightarrow \text{I}_0$  transition can account for the shape of  $\text{Na}^+$  currents elicited by depolarizing pulses in both channel types (Starkus et al., 1997, 1998).

We assumed that the intrinsic rate of channel closing is very fast in the wild-type channel, and much slower ( $>20$ -fold) in the mutant channel. In the mutant channel there is no difference in the rates of the  $\text{O} \rightarrow \text{C}_n$  and the  $\text{R} \rightarrow \text{CI}_n$  transitions, which both represent the closing of the gate in the upper and lower branches, respectively,



and the rate of closing of the wild-type channel when it closes via the lower branch becomes similar to this rate.

In both channel types, the closing of the gate is prevented by cations in the cavity (foot-in-the-door). This is represented on the scheme by the addition of the O+ion and R+ion states, from which there are no backward transitions to the closed states. If the equilibrium between the occupied and the vacant states is shifted toward the former, it will result in slower channel closing. We suggested several mechanisms that can influence the occupancy of the cavity. The most obvious is that increased inward currents provide a constant supply of ions, thereby reducing the duration of vacant periods between ions and the probability of gate closure. In nonpermeating conditions, the electrostatic interaction between the ion in the cavity and the one at the deep site can increase the fraction of vacant periods.

In the wild-type channel, during normal permeation of  $K^+$  there is an extremely high turnover rate of ions in the cavity, so the equilibration between the O and O+ion states is very fast. Although the high occupancy of the cavity during permeation shifts this equilibrium toward the O+ion state, which slows closing considerably compared with its intrinsic rate ( $O \rightarrow C_n$ ), the overall rate of channel closing is fast. In  $Tris^+$ , equilibration between the O and O+ion (and R and R+ion) states is so slow compared with the intrinsic gate closing rate that it solely determines the rate of channel closing and, thus, charge return. Channel closing becomes even slower in  $Tris^+$  conditions in the mutant channel, because the intrinsic rate of gate closure ( $O \rightarrow C_n$  and  $R \rightarrow C_{n-1}$ ) is not much faster than the rate of O – O+ion and R – R+ion equilibration and the two transitions (vacation of the cavity and closing of the gate) are in series.

Why then is channel closing slower during inward permeation of  $K^+$  in the mutant channel when the cavity contains  $K^+$  instead of  $Tris^+$ ? We propose that as in the wild-type channel, cavity occupancy is high during the permeation of  $K^+$  (equilibrium shifted toward O+ion), but because of the low conductance of W434F, the ion turnover rate is much lower than in the wild-type, which results in a slower O – O+ion equilibration and, thus, slows channel closing.

In the wild-type channel, being much faster than the rate-limiting  $C_i \rightarrow C_{i-1}$  transition later in the deactivation pathway, variations in the tail current decay rate have no effect on the rate of charge recovery. The slightly faster recovery rate observed in  $Cs^+$  compared with  $K^+$  or  $Rb^+$  might indicate some direct effect of the ion on the mobile charges of the protein, accelerating the rate-limiting backward  $C_i \rightarrow C_{i-1}$  transition, as it was proposed for  $Ba^{2+}$  (Hurst et al., 1997). In the mutant channel, we assumed that channel closing becomes the rate-limiting step defining the fast component of charge return, which is determined by the interaction

between the ion at the deep site and the one in the cavity. As yet we do not know how the W434F mutation could slow channel closing. Nevertheless, the mutation is drastic enough to almost completely abolish  $K^+$  conduction through the channel, which suggests that it seriously interferes with ion–ion interactions within the pore. It is therefore possible that the electrostatic interaction between the ion at the deep site and the one in the cavity becomes very weak, allowing long dwell times for the ion in the cavity, thereby hindering channel closing. This effect, along with the slowing of the intrinsic gate closing step can explain all the phenomena presented in this paper.

Since the time constant of the slow component of charge recovery was very similar in most cases (18–30 ms), we assumed the rate of the  $I_0 \rightarrow R$  recovery not to be significantly affected by the cations present, and to be fast compared with the  $I_{C1} \rightarrow I_0$  and the  $R \rightarrow C_{n-1}$  transitions. Moreover, we propose that after 15-ms long depolarizations  $I_{C1}$  is the deepest inactivated state that is populated to any significant extent, and that the  $I_{C1} \rightarrow I_0$  transition is rate-limiting in the recovery process, yielding the slow time constant of charge recovery seen in all of these conditions. The fraction of channels that reached the  $I_0$  state was, however, dependent on the ion species, an effect that we assume to be exerted mostly from the external lock-in site. The cations were effective in slowing the  $O \rightarrow I_0$  transition in the following sequence:  $Ba^{2+} \approx Cs^+ > Rb^+ > K^+ > Tris^+ > Na^+$ . As  $Na^+$  is likely to have a higher affinity for the external lock-in site than  $Tris^+$ , yet the weight of the slow component is greater in  $Na^+$  solutions, we propose that  $Na^+$  can also increase the rate of the transition into  $I_0$  by binding to the deep site. This is supported by the experiment shown in Fig. 10, and the fact that barium's effect in  $Na^+_O/Na^+_I$  solution was the complete elimination of the slow component without affecting the fast one.

The transitions into deeper inactivated states are likely to be faster in the wild-type channel than in the mutant. This is indicated by the greater weight of the slow components in the wild-type channel in  $Na^+$  and  $Tris^+$  solutions, and the greater slowing of recovery with extended depolarizing pulses (Figs. 7 and 13).

Due to the fast  $O \rightarrow I_0$  transition in  $Na^+$  solutions, ~60–70% of the channels go beyond the open state during a 15-ms pulse to 0 mV. About half of these then move on to the C-inactivated states, whereas the rest stay in  $I_0$ . In the wild-type channel, a slightly higher fraction reaches the C-inactivated states. Upon repolarization to –100 mV, there should then be three components of the tail current: a fast one from the deactivation of channels from the open state (30–40%), one characterized by an intermediate time constant from channels recovering from  $I_0$  through the lower branch (20–25%), and a slow one characterized by a time con-

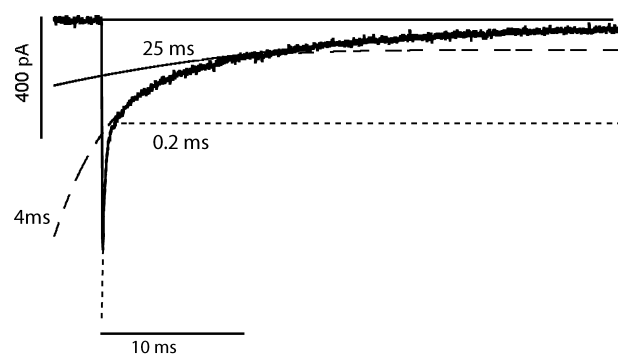


FIGURE 15. The three components of  $\text{Na}^+$  tail currents in the wild-type channel. The trace was recorded in  $115 \text{ Na}^+_{\text{O}}/115 \text{ Na}^+_{\text{I}}$  solutions from an inside out patch containing wild-type channels. The tail current was elicited by stepping back to  $-100 \text{ mV}$  after a  $15\text{-ms}$  long depolarizing pulse to  $0 \text{ mV}$ . The original data trace is shown with the three exponential components of the fit. The short dashed line indicates the fast component ( $\tau = 236 \mu\text{s}$ , channels closing from the open state), the long dashed indicates the intermediate component ( $\tau = 4.3 \text{ ms}$ , channels returning from  $I_0$ ), and the solid line indicates the slow component ( $\tau = 25.5 \text{ ms}$ , channels returning from  $I_{\text{CI}}$ ).

stant of over  $20 \text{ ms}$  from channels recovering from C-inactivated states. These three components can indeed be observed on decaying  $\text{Na}^+$  tail currents through wild-type channels (Fig. 15). Because of the low resolution of charge recovery scatter plots the intermediate component blends into the other two components and cannot be resolved.

In the mutant, the situation is similar in  $\text{Na}^+$  solutions, except the fast tail component is missing due to the low conductance of the open state and the slow  $\text{O} \rightarrow \text{C}_n$  transition. A rising phase of the tail current with a time constant of a few hundred microseconds is seen because of the fast transition to the higher conductance R state from the lower conductance  $I_0$  state. The fast component of recovery is slower than in the wild-type, because the rate-limiting closing transitions here ( $\text{O} \rightarrow \text{C}_n$  and  $\text{R} \rightarrow \text{CI}_n$ ) are slower than the transitions between closed states ( $\text{C}_i \rightarrow \text{C}_{i-1}$ ) that are rate-limiting for channels closing from the open state in the wild-type.

The fact that in both channel types the weight of the slow component in  $\text{Tris}^+$  was smaller than in  $\text{Na}^+$ , but the fast component was significantly slower, suggests that the overall slower recovery in  $\text{Tris}^+$  is due to the prevention of gate closure rather than a higher degree of inactivation.

Barium influences the rate of charge return in a number of ways. First, it hinders entry into the deeper inactivated states, reducing the weight of the slow component. This is most likely exerted from the external lock-in site. Second, it accelerates the closing of the gate by reducing the dwell time of  $\text{Cs}^+$ ,  $\text{Rb}^+$ , and  $\text{K}^+$  in the cavity, but not that of  $\text{Tris}^+$  or  $\text{Na}^+$ . Third, it di-

rectly interacts with the mobile gating charges and speeds up the rate-limiting transition between closed states.

### Conclusions

We have shown here that cations modulate the rate of gating charge recovery in *Shaker* potassium channels through a variety of different mechanisms, acting from different ion binding sites. These effects are very complex and usually several of them occur simultaneously, making unequivocal identification and characterization quite difficult, if not impossible.

One of the important factors through which various ionic conditions modulate the rate of charge return in the mutant channel is the rate of channel closing, which depends on the occupancy of the cavity. This factor is not present in the wild-type channel during normal permeation of  $\text{K}^+$ ,  $\text{Rb}^+$ , or  $\text{Cs}^+$  because, even though permeation significantly slows the closing of the channel, it still remains fast enough not to become rate-limiting in these conditions. The dwell time in the cavity can vary a great deal for different internal cations, even if the deep binding site in the selectivity filter is occupied by the same ion. Such variations may arise from these ions' different interactions with the ion located at the deep site or with the cavity wall, which could be a result of differences in size or hydration energies. The longer dwell time of ions in the cavity of the mutant channel may be the consequence of weakened ion-ion interactions brought on by the altered internal structure of the pore. This effect, along with a slower intrinsic gate closing rate in W434F, may be responsible for the slow closing of this mutant.

Transitions into and recovery from inactivated states also play a major role in determining the rate of charge recovery. One of these seems to be responsible for a slow component present in almost every ionic condition that shows resemblance to the well described slow inactivation mechanism modulated by the occupancy of the external lock-in site. This inactivation mechanism may also be regulated from the deep site, at least in  $\text{Na}^+$  solutions.

We have also found evidence for a direct effect of cations on the gating mechanism, most likely exerted from the deep site, which may be significant only for the divalent barium, but not for monovalent cations.

We constructed a model that can account for most of these effects; however, the characterization of the interactions of cations with the gating mechanism of voltage-gated  $\text{K}^+$  channels is still far from being complete. This study identifies some of these interactions and the ion binding sites they originate from, but other higher resolution methodologies and a more detailed knowledge of the channel structure may be necessary for full understanding of these mechanisms.

We wish to thank M. Hentleff for providing us with WT and W434F, and Marilou Andres, Dan Alicata, and Mary Davis for technical support and assistance. We also wish to thank Dr. Stefan Heinemann for helpful comments on the manuscript.

This study was supported by the National Institutes of Health grant NS21151 to J.G. Starkus.

Submitted: 25 October 2001

Revised: 4 April 2002

Accepted: 5 April 2002

## REFERENCES

- Baukrowitz, T., and G. Yellen. 1995. Modulation of K<sup>+</sup> current by frequency and external [K<sup>+</sup>]: a tale of two inactivation mechanisms. *Neuron*. 15:951–960.
- Baukrowitz, T., and G. Yellen. 1996. Use-dependent blockers and exit rate of the last ion from the multi-ion pore of a K<sup>+</sup> channel. *Science*. 271:653–656.
- Bezánilla, F., E. Perozo, and E. Stefani. 1994. Gating of Shaker K<sup>+</sup> channels: II. The components of gating currents and a model of channel activation. *Biophys. J.* 66:1011–1021.
- Chen, F.S., D. Steele, and D. Fedida. 1997. Allosteric effects of permeating cations on gating currents during K<sup>+</sup> channel deactivation. *J. Gen. Physiol.* 110:87–100.
- Demo, S.D., and G. Yellen. 1992. Ion effects on gating of the Ca(2<sup>+</sup>)-activated K<sup>+</sup> channel correlate with occupancy of the pore. *Biophys. J.* 61:639–648.
- Doyle, D.A., J. Morais Cabral, R.A. Pfueter, A. Kuo, J.M. Gulbis, S.L. Cohen, B.T. Chait, and R. MacKinnon. 1998. The structure of the potassium channel: molecular basis of K<sup>+</sup> conduction and selectivity. *Science*. 280:69–77.
- Fedida, D., N.D. Maruoka, and S. Lin. 1999. Modulation of slow inactivation in human cardiac Kv1.5 channels by extra- and intracellular permeant cations. *J. Physiol.* 515:315–329.
- Harris, R.E., H.P. Larsson, and E.Y. Isacoff. 1998. A permeant ion binding site located between two gates of the Shaker K<sup>+</sup> channel. *Biophys. J.* 74:1808–1820.
- Heinemann, S.H., F. Conti, and W. Stuhmer. 1992. Recording of gating currents from *Xenopus* oocytes and gating noise analysis. *Methods Enzymol.* 207:353–368.
- Hoshi, T., W.N. Zagotta, and R.W. Aldrich. 1991. Two types of inactivation in Shaker K<sup>+</sup> channels: effects of alterations in the carboxy-terminal region. *Neuron*. 7:547–556.
- Hurst, R.S., R. Latorre, L. Toro, and E. Stefani. 1995. External barium block of Shaker potassium channels: evidence for two binding sites. *J. Gen. Physiol.* 106:1069–1087.
- Hurst, R.S., M.J. Roux, L. Toro, and E. Stefani. 1997. External barium influences the gating charge movement of Shaker potassium channels. *Biophys. J.* 72:77–84.
- Iverson, L.E., and B. Rudy. 1990. The role of the divergent amino and carboxyl domains on the inactivation properties of potassium channels derived from the Shaker gene of *Drosophila*. *J. Neurosci.* 10:2903–2916.
- Jiang, Y., and R. MacKinnon. 2000. The barium site in a potassium channel by x-ray crystallography. *J. Gen. Physiol.* 115:269–272.
- Kiss, L., and S.J. Korn. 1998. Modulation of C-type inactivation by K<sup>+</sup> at the potassium channel selectivity filter. *Biophys. J.* 74:1840–1849.
- Korn, S.J., and S.R. Ikeda. 1995. Permeation selectivity by competition in a delayed rectifier potassium channel. *Science*. 269:410–412.
- Levy, D.I., and C. Deutsch. 1996. Recovery from C-type inactivation is modulated by extracellular potassium. *Biophys. J.* 70:798–805.
- Loboda, A., A. Melishchuk, and C. Armstrong. 2001. Dilated and de-funct K channels in the absence of K<sup>+</sup>. *Biophys. J.* 80:2704–2714.
- Loots, E., and E.Y. Isacoff. 1998. Protein rearrangements underlying slow inactivation of the Shaker K<sup>+</sup> channel. *J. Gen. Physiol.* 112:377–389.
- Lopez-Barneo, J., T. Hoshi, S.H. Heinemann, and R.W. Aldrich. 1993. Effects of external cations and mutations in the pore region on C-type inactivation of Shaker potassium channels. *Receptors Channels*. 1:61–71.
- Matteson, D.R., and R.P. Swenson. 1986. External monovalent cations that impede the closing of K channels. *J. Gen. Physiol.* 87:795–816.
- McCormack, K., W.J. Joiner, and S.H. Heinemann. 1994. A characterization of the activating structural rearrangements in voltage-dependent Shaker K<sup>+</sup> channels. *Neuron*. 12:301–315.
- Melishchuk, A., and C.M. Armstrong. 2001. Mechanism underlying slow kinetics of the off gating current in Shaker potassium channel. *Biophys. J.* 80:2167–2175.
- Methfessel, C., V. Witzemann, T. Takahashi, M. Mishina, S. Numa, and B. Sakmann. 1986. Patch clamp measurements of *Xenopus laevis* oocytes: currents through endogenous channels and implanted acetylcholine receptor and sodium channels. *Pflügers Arch.* 407:577–588.
- Neyton, J., and C. Miller. 1988a. Discrete Ba<sup>2+</sup> block as a probe of ion occupancy and pore structure in the high-conductance Ca<sup>2+</sup>-activated K<sup>+</sup> channel. *J. Gen. Physiol.* 92:569–586.
- Neyton, J., and C. Miller. 1988b. Potassium blocks barium permeation through a calcium-activated potassium channel. *J. Gen. Physiol.* 92:549–567.
- Olcese, R., R. Latorre, L. Toro, F. Bezánilla, and E. Stefani. 1997. Correlation between charge movement and ionic current during slow inactivation in Shaker K<sup>+</sup> channels. *J. Gen. Physiol.* 110:579–589.
- Perozo, E., R. MacKinnon, F. Bezánilla, and E. Stefani. 1993. Gating currents from a nonconducting mutant reveal open-closed conformations in Shaker K<sup>+</sup> channels. *Neuron*. 11:353–358.
- Quick, M.W., J. Naeve, N. Davidson, and H.A. Lester. 1992. Incubation with horse serum increases viability and decreases background neurotransmitter uptake in *Xenopus* oocytes. *Biotechniques*. 13:357–361.
- Stampe, P., and T. Begenisich. 1996. Unidirectional K<sup>+</sup> fluxes through recombinant Shaker potassium channels expressed in single *Xenopus* oocytes. *J. Gen. Physiol.* 107:449–457.
- Starkus, J.G., L. Kuschel, M.D. Rayner, and S.H. Heinemann. 1997. Ion conduction through C-type inactivated Shaker channels. *J. Gen. Physiol.* 110:539–550.
- Starkus, J.G., L. Kuschel, M.D. Rayner, and S.H. Heinemann. 1998. Macroscopic Na<sup>+</sup> currents in the “Nonconducting” Shaker potassium channel mutant W434F. *J. Gen. Physiol.* 112:85–93.
- Starkus, J.G., Z. Varga, and M.D. Rayner. 2001. Slow inactivation changes the relationship between channel closing and gating charge return in Shaker potassium channels. *Biophys. J.* 80:218a. (Abstr.)
- Stuhmer, W. 1992. Electrophysiological recording from *Xenopus* oocytes. *Methods Enzymol.* 207:319–339.
- Swenson, R.P., Jr., and C.M. Armstrong. 1981. K<sup>+</sup> channels close more slowly in the presence of external K<sup>+</sup> and Rb<sup>+</sup>. *Nature*. 291:427–429.
- Thompson, J., and T. Begenisich. 2001. Affinity and location of an internal K(+) ion binding site in Shaker K channels. *J. Gen. Physiol.* 117:373–384.
- Varga, Z., M.D. Rayner, and J.G. Starkus. 2001. Ionic current deactivation and gating charge return in slow inactivated Shaker mutants. *Biophys. J.* 80:217a. (Abstr.)
- Wang, Z., and D. Fedida. 2001. Gating charge immobilization caused by the transition between inactivated states in the Kv1.5 channel. *Biophys. J.* 81:2614–2627.
- Wang, Z., J.C. Hesketh, and D. Fedida. 2000. A high-Na(+) conduction state during recovery from inactivation in the K(+) channel Kv1.5. *Biophys. J.* 79:2416–2433.
- Wang, Z., X. Zhang, and D. Fedida. 1999. Gating current studies reveal both intra- and extracellular cation modulation of K<sup>+</sup> channel deactivation. *J. Physiol.* 515:331–339.
- Yang, Y., Y. Yan, and F.J. Sigworth. 1997. How does the W434F mutation block current in Shaker potassium channels? *J. Gen. Physiol.* 109:779–789.